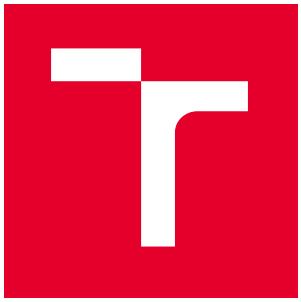

BRNO UNIVERSITY OF TECHNOLOGY

VYSOKÉ UČENÍ TECHNICKÉ V BRNĚ

FACULTY OF MECHANICAL ENGINEERING

FAKULTA STROJNÍHO INŽENÝRSTVÍ

INSTITUTE OF MATHEMATICS

ÚSTAV MATEMATIKY

GEOMETRIC ALGEBRA IN SWITCHED SYSTEMS CONTROL

GEOMETRIC ALGEBRA IN SWITCHED SYSTEMS CONTROL

DOCTORAL THESIS

DIZERTAČNÍ PRÁCE

AUTHOR — Ing. Anna Derevianko

AUTOR PRÁCE

SUPERVISOR — doc. Mgr. Petr Vašík, Ph.D.

ŠKOLITEL

BRNO 2024

Abstract

In this thesis, the controllability of 2×2 switched systems with regular matrices is investigated by means of Geometric Algebra for Conics (GAC) as a mathematical framework for analysis and optimization of control strategies. The research demonstrates the efficiency of GAC in the construction of switching points and paths while minimizing the number of switches and numerical errors.

Classification of controllability is provided based on the geometric properties of particular switched systems. For controllable switched systems, the controlling algorithm based on the GAC primitives is introduced in which the symbolic algebra operations are used, more precisely the wedge and inner product. Therefore, no numerical solver to the system of equations is needed. Indeed, the only operation that may bring in a numerical error is a vector normalisation, ie., square root calculation. The proposed approach creates possibility of passing from the classical solution of the controllability problem for switched systems to a geometric one, based on the type of phase trajectory.

Keywords

switched system, geometric algebra, controllability, Clifford algebra

Abstrakt

V této práci je zkoumána řiditelnost switched systémů 2×2 s regulárními maticemi pomocí Geometrické algebry pro kuželosečky (GAC). Je provedena analýza a optimalizace switched strategií. Výzkum ukazuje účinnost GAC při hledání switching bodů a minimalizaci jejich počtu při maximálním omezení numerických chyb.

Na základě geometrických vlastností konkrétních switched systémů je uvedena klasifikace jejich řiditelnosti. Pro řiditelné switched systémy je představen algoritmus na hledání switching cest založený na kuželosečkách reprezentovaných v GAC, v němž jsou použity operace symbolické algebry, přesněji vnější a vnitřní součin. Není tedy zapotřebí numerického řešení soustavy rovnic. Jedinou operací, která může vnést numerickou chybu, je normalizace vektoru, tedy výpočet odmocniny. Navržený přístup vytváří možnost přejít od klasického řešení problému řiditelnosti pro switched systémy ke geometrickému řešení založenému na typu fázové trajektorie.

Klíčová slova

switched systém, geometrická algebra, řiditelnost, Cliffordova algebra

Declaration

I hereby declare that my doctoral thesis topic on the theme of ”Geometric Algebra in Switched Systems Control” represents my own work under the guidance of supervisor, and has not been previously included in a thesis or dissertation submitted to this or any other institution for a degree, diploma or other qualifications.

20. 4. 2024 Ing. Anna Derevianko

Preface

I would like to thank my supervisor doc. Mgr. Petr Vašík, Ph.D. for the excellent guidance and support during this process. I also wish to thank all of the respondents, without whose cooperation I would not have been able to perform this analysis.

Ing. Anna Derevianko

Contents

Introduction **8**

1 Geometric algebras **10**
1.1 Grassmann Algebras 11
1.2 Clifford Algebras 12
1.3 Introduction to Geometric Algebras 14
1.4 Conformal Geometric Algebra 15
1.5 Compass Ruler Algebra 16
1.6 Geometric Algebra for Conics 18
1.6.1 GAC objects description 21
1.6.2 Parameter extraction 23
1.6.3 Transformations 24
1.6.4 Intersections and contact points in GAC 26
1.7 QC2GA 33
1.8 Summary of Chapter 1 33

2 Switched systems **35**
2.1 Dynamical system 35
2.2 Basic theory of switched systems 37
2.3 Standard methods 39
2.3.1 Nullclines 40
2.3.2 Solution as a parametrized curve 42
2.4 Types of 2x2 linear systems depending on equilibrium point 43
2.5 Summary of Chapter 2 44

3 Control of the switched system by means of GAC **45**
3.1 Center-Center 45
3.2 Algorithm for a switching path construction 47

3.3 Examples and comparison to the numerical methods . . . 49
3.4 Saddle-Saddle . . . 55
3.5 Center-Saddle . . . 57
3.6 Node-Node . . . 58
3.6.1 Stable Node . . . 59
3.6.2 Unstable Node . . . 61
3.6.3 Stable-Unstable Nodes . . . 62
3.6.4 Dicritical Node . . . 63
3.7 Center-Node . . . 64
3.8 Summary of Chapter 3 . . . 65

4 Cases laying out of GAC **66**
4.1 Focus-Focus . . . 66
4.1.1 Unstable Focus . . . 68
4.1.2 Stable Focus . . . 68
4.1.3 Stable-Unstable Focus . . . 69
4.2 Saddle-Focus . . . 71
4.3 Node-Focus . . . 72
4.4 Summary of Chapter 4 . . . 72

5 Results **74**

6 Conclusions **75**

Introduction

Switched systems form a special case of hybrid dynamical systems with both discrete and continuous dynamics, which are described by a differential equation and a state machine or automaton, respectively. They are widely applied in the cases where a real system cannot be described by one single model. Numerous examples are given by engineering systems of electronics, power systems, traffic control and others, [1]. Since the 1990s, research of switched systems stability has become very popular, see e.g. [2, 3]. The particular case of linear switched systems was considered by Patrizio Colaneri in [4]. More modern literature about switched systems is represented by the works of Yuan Lin, Yuan Sun-Ge Wang, and Jiang-Wang [5], Zhong-Ping, Yuan Wang [6]; the question of stability remains relevant until today.

Another topic related to switched systems is controllability. Nowadays, the most popular approach in searching for a control of a switched system is connected with generalizations of Kalman condition, [7] and Lyapunov functions, [8], which requires complex algorithmic structures. Applications of optimal control for switched dynamical systems can be found in various fields, including robotics, power systems, autonomous vehicles, and manufacturing systems, where systems exhibit complex behavior arising from the interaction between continuous dynamics and discrete events, [9].

The ordinary Lyapunov function is used to test whether a given dynamical system is stable (more precisely asymptotically stable), but does not provide any information about controllability. Particular specificity of switched systems is in the interaction between the continuous variable and the discrete state, which is not present in the standard control systems. In the works of D. Liberzon [10, 11], the author addresses the problems of stability and control for particular types of switched systems, using the analytical approach, ie., Lyapunov function and Brockett's condition for asymptotic stability by continuous feedback and controllability. The stabilization problem for switched positive regular linear systems by

state-dependent switching was considered in [12] and anti-bump switching control problem was introduced in [13]. The case of linear switched singular systems is studied, e.g. in [3].

The issue of optimal control has also been addressed several times. The most popular are problems of time- or distance-optimality. For example, finding time-optimal control for dynamical system was considered by Nasir Uddin Ahmed [14] while for switched systems analogical problem was considered in [15], where the author constructs a minimizing sequence and uses compactness property for finding subsequence that minimizes the cost functional. Another way of optimization is construction of a switching path with minimal amount of switches which is of our particular interest.

The novelty of this thesis lies in using Geometric Algebra (GA) for investigation of the switched systems controllability. Geometric Algebra offers a powerful mathematical framework for handling geometric operations with elegance and efficiency. Originating from Grassmann algebras and Clifford algebras, GA unifies geometric primitives and transformations within a single algebraic structure, providing a seamless approach to geometric analysis and manipulation.

Geometric Algebra for Conics (GAC) is an efficient geometric tool to handle both conics and their transformations as elements of a particular Clifford algebra, [16], [17], [18].

The thesis is structured in the following way.

First chapter describes the fundamental concepts of Grassmann and Clifford algebras, highlighting their role in forming the basis of Geometric Algebra.

Second chapter deals with description of switched systems, their place in the theory of dynamical systems, and controllability.

Third chapter deals with the 2×2 switched systems with the special type subsystems. More precisely, those subsystems that have a specific equilibrium point and trajectories intrinsic to Geometric Algebra for Conics. Let us stress that in the Euclidean space, the problem of finding intersection points of two conics is reduced to solving the system of quadratic equations using numerical methods. To avoid the use of the numerical solver we use Geometric Algebra for Conics and demonstrate it on various examples.

Fourth chapter describes the controllability of the 2×2 switched systems with regular matrices of each subsystem, whose phase trajectories are not conic sections.

We shall demonstrate our results on examples of specific switched systems. We provide outputs of our implementation in Python using a module Clifford for GAC operations.

Chapter 1

Geometric algebras

Geometric Algebra (GA) and its special types, such as Compass Ruler Algebra (CRA) and Geometric Algebra for Conics (GAC), provide powerful mathematical frameworks for handling geometric operations in a unified manner. Originating from Grassmann and Clifford algebras, GA offers a rich algebraic structure that encapsulates geometric primitives and transformations within a single framework. In this chapter, we outline the fundamental concepts of Grassmann and Clifford algebras before dealing with the applications and extensions provided by GA.

Clifford algebras extend Grassmann algebras by incorporating geometric interpretations through the Clifford product. By unifying the outer product and the dot product into a single geometric product, Clifford algebras provide a framework for geometric operations.

Let us start from introducing the concept of Tensor algebra for better understanding of the consequent description of Clifford algebras.

Definition 1.0.1. Let V be a vector space over a field $\mathbb{R}$. The tensor algebra of V, denoted by $T(V)$, is defined as the direct sum of all tensor products of V with itself:

$$T(V) = \bigoplus_{n=0}^{\infty} V^{\otimes n}$$

where $V^{\otimes n}$ represents the n-fold tensor product of V with itself. The elements of $T(V)$ are called tensors. The direct sum ensures that $T(V)$ contains tensors of all orders, from scalars (order 0) to higher-order tensors, [19].

The following section deals with Grassmann algebras, also known as exterior algebras, which are a type of associative algebra, that includes antisymmetric products.

1.1 Grassmann Algebras

Given a vector space V, the Grassmann algebra $\Lambda(V)$ associated with V is constructed by taking the quotient of the tensor algebra over V by the ideal generated by the antisymmetrization of tensor products:

$$\Lambda(V) = T(V)/I$$

where $T(V)$ is the tensor algebra of V and I is the ideal generated by

$$v \wedge w + w \wedge v$$

for all $v, w \in V$, where $\wedge$ denotes the outer product. The resulting algebra $\Lambda(V)$ contains elements called outer products, which capture the antisymmetric properties of geometric quantities.

The connection between the outer product and vector product becomes evident when considering their geometric interpretations in terms of oriented volumes. The outer (cross) product of two vectors in three dimensions results in a vector that is perpendicular to both input vectors. It can be expressed as:

$$\boldsymbol{a} \times \boldsymbol{b} = \boldsymbol{c}.$$

Grassmann's outer product (usually denoted as $\wedge$)

$$\boldsymbol{a} \wedge \boldsymbol{b} = \Omega$$

can be represented as the geometric interaction between two vectors, wherein one vector moves along the other to create a directed area. The newly formed object is neither a vector nor a scalar; instead, it is referred to as a bivector, represents the oriented area of the parallelogram spanned by the two vectors.

Hodge duality relates these two operations by expressing the cross product in terms of the wedge product:

$$\boldsymbol{a} \times \boldsymbol{b} = \star(\boldsymbol{a} \wedge \boldsymbol{b})$$

where $\star$ denotes the Hodge star operator, which maps an n-form to an n-form by taking the wedge product of a given form with the appropriate volume form. In three dimensions, this operation converts a 2-form (bivector) to a 1-form (vector), and vice versa.

Similarly, the outer product of the bivector with another vector results in the creation of a directed volume, identified as a trivector. The process can be extended to form an n-volume, which will be refered to as a n-vector.

In the following we recall a concept of Clifford algebra and its connection with quaternions.

1.2 Clifford Algebras

The connection between Clifford algebras and Grassmann algebras arises from the fact that Clifford algebras contain Grassmann algebras as subalgebras, together with the antisymmetric product. Specifically, for a vector space V, the exterior product of vectors in $\Lambda(V)$ is embedded into the corresponding Clifford algebra $\mathcal{C}l(V)$.

Given a real vector space V equipped with an quadratic form $Q(\mathbf{v})$, the Clifford algebra $\mathcal{C}l(V)$ associated with V is constructed as the quotient space:

$$\mathcal{C}l(V) = T(V)/I,$$

where $T(V)$ is the tensor algebra of V and I is the ideal generated by $v \otimes v - Q(\mathbf{v})\mathbf{1}$ for all $v \in V$, where $\mathbf{1}$ denotes the scalar element of the basis of $T(V)$. The product in the algebra is called the Clifford product. The ideal ensures that the elements of the Clifford algebra square to scalars. The resulting algebra $\mathcal{C}l(V)$ contains elements called multivectors.

Let us note that the outer-product is anti-commutative and associative giving $a \wedge b = -(b \wedge a)$ and $a \wedge (b \wedge c) = (a \wedge b) \wedge c = a \wedge b \wedge c$. Grassmann's outer product was unified by Clifford and into one geometric product such that $ab = a \cdot b + a \wedge b$, where $\cdot$ represents the dot or inner product.

Alternatively, Clifford Algebra can be defined as the associative algebra generated by the vectors in a vector space V, equipped with a quadratic form $Q : V \to \mathbb{R}$, with the relations:

$$vw + wv = 2Q(v, w),$$

for all $v, w \in V$.

In this terms the Clifford product of two vectors v and w is defined as:

$$v \wedge w = \frac{1}{2}(vw - wv).$$

It represents the antisymmetric part of the product of v and w and is a fundamental operation in geometric algebra.

Remark. Signature (p, q) of Clifford algebra $\mathcal{C}l(p, q)$ denotes that algebra contains p base vectors that square to $+1$ and q vectors that square to -1.

Let V be a n-dimensional Euclidean space, while p-subspace is a subspace of dimension p. For a multivector $M \in \bigwedge V$, $\quad < M_i >_p \in \bigwedge_p V$ denotes its component of grade p. p-blade is multivector $B = v_1 \wedge \cdots \wedge v_p \in \bigwedge_p V$, with $v_1, \ldots, v_p \in \bigwedge V$. Note, that a scalar is a 0-blade, for more details see [20].

Let us now consider the example describing the connection between Clifford algebra and quaternions.

Example 1. The Clifford algebra $\mathcal{C}l(3,0)$ of the pure imaginary quaternions is a real associative algebra generated by a three-dimensional vector space spanned by the basis elements $\{1, e_1, e_2, e_3, e_1e_2, e_2e_3, e_1e_3, e_1e_2e_3\}$. These basis elements satisfy the following multiplication rules:

$$e_ie_j + e_je_i = 2\delta_{ij},$$

where δ_{ij} is the Kronecker delta, which equals 1 if $i = j$, and 0 otherwise. The elements of $\mathcal{C}l(3,0)$ can be represented as sums of scalars and products of basis elements, such as $a+be_1+ce_2+de_3+(fe_1e_2+ge_2e_3+he_3e_1)$, where a, b, c, d, f, g, h are real scalars.

Now consider the quadratic form $Q = (I)$.

A general quaternion can be written as $q = a + bi + cj + dk$, where a, b, c, d are real numbers and i, j, k satisfy the following: $i^2 = j^2 = k^2 = -1, \quad ijk = -1$.

Let us consider the $3D$ Euclidean space with basis vectors e_1, e_2, e_3. The imaginary unit can be identified in Clifford algebra as one of the 2-blades $e_1 \wedge e_2; e_1 \wedge e_3; e_2 \wedge e_3$, spanned by the three Euclidean basis vectors e_1, e_2, e_3. We choose $i = e_1e_2$. Anticommutativity follows, ie., $e_1e_2 = -e_2e_1$. Then

$$i^2 = (e_1e_2)^2 = e_1e_2e_1e_2 = -e_1e_2e_2e_1 = -e_1e_1 = -1.$$

Analogically, $j = e_2e_3$, $k = e_1e_3$ and

$$ijk = e_1e_2e_2e_3e_1e_3 = -e_1e_1 = -1.$$

Using this notation, we can express the quaternion rotation operator by angle θ as a linear combination of the basis elements:

$$R(\theta) = \cos(\frac{\theta}{2}) + \sin(\frac{\theta}{2})(bi + cj + dk),$$

where $q = bi + cj + dk$ is a unit quaternion representing the axis of rotation.

The fundamental transformation in Clifford algebra is reflection. The given vectors $a, n \in \mathcal{C}l(3,0)$, the reflection of a in n is given by $a' = nan^{-1}$, where n is a non-null 1-vector. It is well known that Euclidean transformations, such as rotation and translation, are generated by reflection, see [21].

Remark (Rotor). Given two unit vectors $m, n \in \mathbb{S}^2 \subset \mathbb{R}^3$, where $\mathbb{S}^2$ denotes a unit sphere. The consecutive reflection of vector a in vectors n and m can be written as $a' = mnan^{-1}m^{-1}$, see Figure 1.1

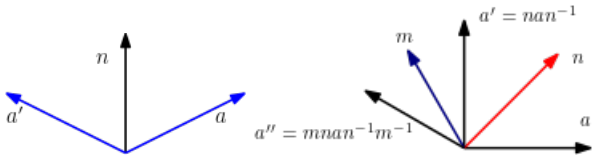

Figure 1.1: Reflection and Rotation generated by two reflections

$$v' = T(\theta, t) \cdot v \cdot R^{-1}(\theta, t).$$

We shall use the term Geometric Algebra to mean the coupling of Clifford algebras with an accompanying geometric interpretation.

1.3 Introduction to Geometric Algebras

Geometric algebra (GA) is a Clifford algebra with a specific embedding of Euclidean space (of arbitrary dimension) in such a way that the intrinsic geometric primitives as well as their Euclidean transformations are viewed as elements of a single vector space, precisely vectors and bivectors, respectively. This concept was introduced by D. Hestenes in [22] and has been used in many mathematical and engineering applications since, see e.g. [23, 24]. The computational advantage of GA lays in that geometric operations, such as intersections, tangents, distances, etc., are linear functions and can therefore be calculated efficiently. To show this, we refer to [21] for the basics of geometric algebras, especially for the conformal representation of Euclidean space. 3D Euclidean space is actually represented in Clifford's algebra $\mathcal{C}l(4,1)$, and the consequent geometric algebra is often denoted as $\mathbb{G}_{4,1}$ with spheres of all types as geometric primitives and Euclidean transformations at hand, see e.g. [25]. In the following work the two-dimensional subalgebra $\mathbb{G}_{3,1}$ is also considered. It is called the Compass Ruler Algebra (CRA), [26], which is an analogue of $\mathbb{G}_{4,1}$ for two-dimensional Euclidean space.

Basic elements of n-dimensional Geometric Algebra are represented by blades with grades $0, 1, 2, \ldots, n$, where a scalar is considered as a 0-blade and the 1-blades are the basis vectors $e_1; e_2; \ldots; e_n$. The 2-blades $e_i \wedge e_j$ are blades constructed by two 1-blades, and so on. There exists the only one element of the maximum grade n, $I = e_1 \wedge e_2 \wedge \cdots \wedge e_n$, that is called a pseudoscalar. The products in Geometric Algebra are presented by the outer, the inner and the geometric product, see [26].

Geometric primitives in Geometric Algebra have two algebraic representations, the IPNS (inner product null space) and the OPNS (outer product null space)

representation. These representations are duals of each other.

Let $E \subset \mathbb{R}^3$ be one of the geometric entity listed above then we say that a multivector E_{IPNS} is an inner product null space representation of E if

$$\{x \in \mathbb{R}^3 : P(x) \cdot E_{IPNS} = 0\} = E,$$

ie., it is possible to represent a subspace with a blade as the set of all vectors having a zero contraction with the blade. This method is called the Inner Product Null Space (IPNS) representation of subspaces.

Analogously we say that a multivector E_{OPNS} (a dual of E) is an outer product null space representation of E if

$$\{x \in \mathbb{R}^3 : P(x) \wedge E_{OPNS} = 0\} = E,$$

ie., any vector having zero outer product with a blade is inside its subspace. This is called the Outer Product Null Space (OPNS) representation of subspaces.

Further we provide a brief theoretical survey of geometric algebras.

1.4 Conformal Geometric Algebra

Conformal Geometric Algebra (CGA) is a conformal model of an n–dimensional Euclidean space. It is a Clifford algebra of signature $(n+1, 1)$ denoted as $\mathcal{C}l(n+1, 1)$ together with a specific embedding of a Euclidean point which be described for the case $n = 2$ in the following Section. As a result, CGA contains representatives of Euclidean primitives as well as their transformations. Moreover, spheres of dimension up to $n - 1$ can be represented and some non–Euclidean transformations such as scaling may be performed. Let us just note that to unify the object representation, one can consider Euclidean primitives as specific spheres, e.g., a line is one–dimensional sphere with infinite radius. Let us add that this model allows simple construction of objects by wedge product of generating points (OPNS representation), parameter extraction (IPNS representation) and intersections (wedge of IPNS representations).

In the following Section, a conformal model of two–dimensional Euclidean space called Compass Ruler Algebra (CRA) is recalled as well as all necessary objects, transformations and operations.

1.5 Compass Ruler Algebra

The Compass Ruler Algebra (CRA) is the Conformal Geometric Algebra in 2D. Let us remind the main notations (see Table 1.1) and elements of CRA. The algebra contains two Euclidean basis vectors e_1 and e_2 of the plane and two additional basis vectors e_+, e_- with positive and negative signatures, respectively, which means that they square to +1 as usual (e_+) and to -1 (e_-). Let us consider the alternative basis, containing

$$e_0 = \frac{1}{2}(e_- + e_+), \quad e_\infty = e_- - e_+,$$

with the geometric meaning that e_0 represents the 2D origin, e_∞ represents the infinity.

Notation	Meaning
e_1, e_2	2D basis vectors
e_0	origin
e_∞	infinity
AB	geometric product of A and B
$A \wedge B$	outer product of A and B
$A \cdot B$	inner product of A and B
A^*	dual of A
A^{-1}	inverse of A

Table 1.1: Notations of Compass Ruler Algebra

Let us now consider geometric meaning of a point P with 2D coordinates (x_1, x_2) and its IPNS representation as its null space with respect to the inner product should be computed.

$$x = x_1 e_1 + x_2 e_2$$

is extended to a 4D vector by taking a linear combination of the 4D basis vectors e_1, e_2, e_∞, and e_0:

$$P = x + \frac{1}{2}x^2 e_\infty + e_0,$$

where x^2 is the inner product:

$$x^2 = (x_2 e_1 + x_2 e_2) \cdot (x_2 e_1 + x_2 e_2) = x_1^2 e_1^2 + 2x_1 x_2 (e_1 \cdot e_2) + x_2^2 e_2^2 = x_1^2 + x_2^2.$$

Therefore, we can consider the embedding:

$$E_2 \hookrightarrow \mathbb{R}^{3,1} \hookrightarrow \mathcal{C}l(V).$$

In the Compass Ruler Algebra exists a correspondence between algebraic expressions and geometric objects such as circles and lines. Circles, for instance, can be defined based through three points. This is the reason why the circumscribed circle of a triangle can be expressed easily. Furthermore, with the help of the products of the algebra, distances and angles as well as geometric operations such as intersections of geometric objects can be described [26].

In geometric algebra, the intersection of geometric entities can be expressed using the wedge product of their respective IPNS representations, [25].

Let us now consider basic elements.

To describe circle, we use center point P and its radius r:

$$C = P - \frac{1}{2}r^2 e_\infty,$$

that can be rewritten as

$$C = x + \frac{1}{2}x^2 e_\infty + e_0 - \frac{1}{2}r^2 e_\infty$$

or

$$C = x + \frac{1}{2}(x^2 - r^2)e_\infty + e_0.$$

It is evident that point can be represented as a circle of radius zero. A circle can also be described with the help of three points that lie on it, by

$$C^* = P_1 \wedge P_2 \wedge P_3.$$

The other widely used in CRA object is a point pair, that can be defined as intersection of two circles:

$$Pp = C_1 \wedge C_2$$

and in OPNS representation:

$$Pp^* = P_1 \wedge P_2.$$

A line in CRA is defined by

$$L = n + de_\infty,$$

where $n = n_1 e_1 + n_2 e_2$ refers to the 2D normal vector of the line L and d is the distance to the origin. A line can also be defined with the help of two points that lie on it and the point at infinity: $L = P_1 \wedge P_2 \wedge e_\infty$. Line can be also considered as a circle of infinite radius.

1.6 Geometric Algebra for Conics

Now let us consider Geometric Algebra for Conics (GAC), that is the generalization of $\mathbb{G}_{4,1}$, proposed by C. Perwass, [21], and J. Hrdina, A. Návrat, P. Vašík, [16]. Let us stress that in the current work the notation of [16] is used, ie., $\bar{n}$ and n are taking place of e_0 and e_∞, respectively. In the usual basis $\bar{n}, e_1, e_2, n$, the embedding of a plane into $\mathbb{G}_{3,1}$ is given by

$$(x, y) \mapsto \bar{n} + xe_1 + ye_2 + \frac{1}{2}(x^2 + y^2)n,$$

where e_1, e_2 form the Euclidean basis and $\bar{n}$ and n stand for a specific linear combination of additional basis vectors e_3, e_4 with $e_3^2 = 1$ and $e_4^2 = -1$, giving them the meaning of the coordinate origin and infinity, respectively, [21].

Considering the coefficients from thee CRA part, ie., $1, x, y, x^2 + y^2$, we can note that they belong to the basis for polynomial of degree 2 of 2 variables. In order to cover general conics, which are described by the polynomial of degree 2 of 2 variables, it is necessary to add two terms: $\frac{1}{2}(x^2 - y^2)$ and xy, for which it is needed to introduce two new infinities, [27]. Therefore, we form two additional Witt pairs. Thus the resulting number of generating vectors of Geometric Algebra for Conics is equal to eight.

Analogously to the notation in [21], the corresponding basis elements are denoted as

$$\bar{n}_+, \bar{n}_-, \bar{n}_\times, e_1, e_2, n_+, n_-, n_\times. \tag{1.1}$$

This notation suggests that the basis elements e_1, e_2 play the usual role of standard basis of the plane while the null vectors $\bar{n}$, n represent the origin and infinity, respectively. Note that there are three orthogonal 'origins' $\bar{n}$ and three corresponding orthogonal 'infinities' n [16]. In terms of this basis, a point of the plane $\mathbf{x} \in \mathbb{R}^2$ defined by $\mathbf{x} = xe_1 + ye_2$ is embedded using the operator $\mathcal{C} : \mathbb{R}^2 \to \mathcal{C}one \subset \mathbb{R}^{5,3}$, which is defined by

$$\mathcal{C}(x, y) = \bar{n}_+ + xe_1 + ye_2 + \frac{1}{2}(x^2 + y^2)n_+ + \frac{1}{2}(x^2 - y^2)n_- + xyn_\times. \tag{1.2}$$

Definition 1.6.1. Geometric Algebra for Conics (GAC) is the Clifford algebra $\mathbb{C}l(5, 3)$ together with the embedding (1.2) in the basis (1.1).

Note that, up to the last two terms, the embedding (1.2) is the embedding of the plane into the two-dimensional conformal geometric algebra $\mathbb{G}_{3,1}$. In particular, it

Notation	Meaning
e_1, e_2	2D basis vectors
$\bar{n}_+, \bar{n}_-, \bar{n}_\times$	origins
$n_+, n_-, n_\times$	infinities
AB	geometric product of A and B
$A \wedge B$	outer product of A and B
$A \cdot B$	inner product of A and B
A^*	dual of A
A^{-1}	inverse of A

Table 1.2: Notations of Geometric Algebra for Conics

is evident that the scalar product of two embedded points is the same as in $\mathbb{G}_{3,1}$, ie., for two points $\mathbf{x}, \mathbf{y} \in \mathbb{R}^2$ we have

$$\mathcal{C}(\mathbf{x}) \cdot \mathcal{C}(\mathbf{y}) = -\frac{1}{2}\|\mathbf{x} - \mathbf{y}\|^2, \tag{1.3}$$

where the standard Euclidean norm is considered on the right hand side. This demonstrates the linearisation of distance problems. In particular, each point is represented by a null vector. Let us recall that the invertible algebra elements are called versors and they form a group, the Clifford group, and that conjugations with versors give transformations intrinsic to the algebra. Namely, if the conjugation with a $\mathbb{G}_{5,3}$ versor R preserves the set $\mathcal{C}one$, ie., for each $\mathbf{x} \in \mathbb{R}^2$ there exists such a point $\bar{\mathbf{x}} \in \mathbb{R}^2$ that

$$R\mathcal{C}(\mathbf{x})\tilde{R} = \mathcal{C}(\bar{\mathbf{x}}), \tag{1.4}$$

where $\tilde{R}$ is the reverse of R, then $\mathbf{x} \to \bar{\mathbf{x}}$ induces a transformation $\mathbb{R}^2 \to \mathbb{R}^2$ which is intrinsic to GAC. See [16] to find that the conformal transformations are intrinsic to GAC.

Let us also recall the outer (wedge) product, inner product and the duality

$$A^* = AI^{-1}, \tag{1.5}$$

where $I = e_{12345678}$ is a pseudoscalar, i.e the highest grade element.

For our purposes, we stress that these operations correspond to sums and products only. Thus, computational error is minimized. Indeed, the wedge product is calculated as the outer product of vectors on each vector space of the same grade blades, while the inner product acts on these spaces as the scalar product. The

extension of both operations to general multivectors adds no computational complexity due to linearity of both operations.

Let us also recall that if a conic C is considered as a wedge of five different points (which determine a conic uniquely), the appropriate 5-vector E^* is called an outer product null space representation (OPNS) and its dual E, indeed a 1-vector, is called the inner product null space (IPNS) representation. The reason is that if a point P lies on a conic C then

$$P \cdot E = 0 \quad \text{and} \quad P \wedge E^* = 0.$$

Consequently, intersections of two geometric primitives are given as the wedge product of their IPNS representations, ie.,

$$C_1 \cap C_2 = E_1 \wedge E_2$$

for two conics C_1, C_2 and their IPNS representations E_1 and E_2, respectively, see [16].

Let us describe the inner product representation more precisely. An element $A_I \in \mathbb{G}_{5,3}$ is the inner product representation of a geometric object A in the plane if and only if $A = \{\mathbf{x} \in \mathbb{R}^2 : \mathcal{C}(\mathbf{x}) \cdot A_I = 0\}$. The representable objects can be found by examining the inner product of a vector and an embedded point. A general vector in the conic space $\mathbb{R}^{5,3}$ in terms of our basis is of the form

$$v = \bar{v}^+ \bar{n}_+ + \bar{v}^- \bar{n}_- + \bar{v}^\times \bar{n}_\times + v^1 e_1 + v^2 e_2 + v^+ n_+ + v^- n_- + v^\times n_\times$$

and its inner product with an embedded point is then given by

$$\mathcal{C}(x,y) \cdot v = -\frac{1}{2}(\bar{v}^+ + \bar{v}^-)x^2 - \bar{v}^\times xy - \frac{1}{2}(\bar{v}^+ - \bar{v}^-)y^2 + v^1 x + v^2 y - v^+,$$

ie., by a general polynomial of degree two. Thus the objects representable in GAC are exactly conics. We also see that the two-dimensional subspace generated by infinities $n_-, n_\times$ is orthogonal to all embedded points. In other words, the inner representation of a conic in GAC can be defined as a six–dimensional vector

$$Q_I = \bar{v}^+ \bar{n}_+ + \bar{v}^- \bar{n}_- + \bar{v}^\times \bar{n}_\times + v^1 e_1 + v^2 e_2 + v^+ n_+ \tag{1.6}$$

with coefficients $(\bar{v}^+, \bar{v}^-, \bar{v}^\times, v^1, v^2, v^+)$.

1.6.1 GAC objects description

The classification of conics is well known. There exists 3 types of non–degenerate conics: ellipse, hyperbola, and parabola. Let us briefly describe inner product representations of the conics in GAC. More information can be found in [16]. Let us present the vector form (1.6) appropriate to each conic type in the simplest case, ie., an axes–aligned conic with its centre in the origin. The results may be verified easily by multiplying each vector by an embedded point. For instance, an axes–aligned ellipse E_I with semi–axes a, b and center in the coordinate system origin is a vector of the form

$$E_I = (a^2 + b^2)\bar{n}_+ + (a^2 - b^2)\bar{n}_- - a^2b^2n_+.$$

An ellipse and hyperbola E with the semi–axes a, b centred in $(u, v) \in \mathbb{R}^2$ rotated by angle θ in the GAC IPNS representation are given by

$$\begin{aligned} E_I = {} & \bar{n}_+ - (\alpha\cos 2\theta)\bar{n}_- - (\alpha\sin 2\theta)\bar{n}_\times \\ & + (u + u\alpha\cos 2\theta - v\alpha\sin 2\theta)e_1 + (v + v\alpha\cos 2\theta - u\alpha\sin 2\theta)e_2 \\ & + \tfrac{1}{2}\left(u^2 + v^2 - \beta - (u^2 - v^2)\alpha\cos 2\theta - 2uv\alpha\sin 2\theta\right)n_+, \end{aligned} \tag{1.7}$$

where

$$\alpha = \frac{a^2 - b^2}{a^2 + b^2}, \quad \beta = \frac{2a^2b^2}{a^2 + b^2}$$

for an ellipse and

$$\alpha = \frac{a^2 + b^2}{a^2 - b^2}, \quad \beta = \frac{-2a^2b^2}{a^2 - b^2}$$

for a hyperbola, see Figure 1.2. In the case of parabola we have with the semi-latus

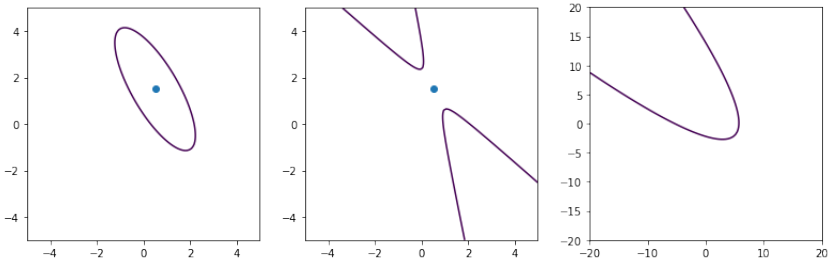

Figure 1.2: Ellipse, Hyperbola and Parabola

rectum p centred in $(u, v) \in \mathbb{R}^2$ rotated by angle θ we have:

$$\begin{aligned} P_I = {} & \bar{n}_+ + \cos 2\theta \bar{n}_- + \sin 2\theta \bar{n}_\times \\ & + (u + u\cos 2\theta + v \sin 2\theta - 2p \sin\theta) e_1 \\ & + (v - v\cos 2\theta + u \sin 2\theta + 2p \cos\theta) e_2 \\ & + \tfrac{1}{2}\left(u^2 + v^2 + (u^2 - v^2)\cos 2\theta + 2uv \sin 2\theta - 4pu \sin\theta + 4pv\cos\theta\right) n_+, \end{aligned} \tag{1.8}$$

It is also visualized in Figure 1.2.

Let us recall the circle representation in GAC. More information can be found in [16].

Proposition 1.6.1. A circle C centred in (p_1, p_2) with radius ρ is given by

$$C_I = \bar{n}_+ + p_1 e_1 + p_2 e_2 + \tfrac{1}{2}(p_1^2 + p_2^2) n_+ - \tfrac{1}{2}\rho^2 n_+$$

.

Though a line is not an element of GAC, it still can be represented: line L with unite normal (n_1, n_2) and a shift d from the origin is given by

$$L_I = n_1 e_1 + n_2 e_2 + d n_+.$$

Remark. Let us note that a single line in GAC is not an intrinsic primitive and thus we may understand it as a CRA object, [16]. Therefore its IPNS representation has the same form as in CRA, [26],

$$n_1 e_1 + n_2 e_2 + d n_+$$

where $n = (n_1, n_2)$ is the normal vector and d is the distance from coordinate origin. The OPNS representation of a line passing through two points p_1 and P_2 is, [16] of the form

$$P_1 \wedge P_2 \wedge n_+ \wedge n_- \wedge n_\times.$$

Formulas for these degenerate conics can be also derived from the non–degenerate ones by means of certain limits [16].

Proposition 1.6.2. GAC inner representation of two parallel lines is given by (1.7) with coefficients $\alpha = -1, \beta = 2a^2$, where $2a$ is the distance between the lines. GAC inner representation of two intersecting lines, which are not perpendicular, is given by (1.7) with coefficients $\alpha = \frac{1+k^2}{1-k^2}, \beta = 0$, where k is the line derivation.

Note that parallel lines are obtained from an ellipse by the limit $b \to \infty$. The intersecting lines are obtained from a hyperbola by setting $b = ka$ and then by taking the limit $a \to 0$, [16].

Two perpendicular lines cannot be expressed in the form (1.7) since the coefficient of $\bar{n}_+$ has to be zero, see [28]. For this particular case we get the GAC inner representation of the form

$$\begin{aligned} LL_I^{\perp} = &-(\alpha\cos 2\theta)\bar{n}_- - (\sin 2\theta)\bar{n}_\times + (u\cos 2\theta - v\sin 2\theta)e_1 \\ &+ (v\cos 2\theta - u\sin 2\theta)e_2 - \tfrac{1}{2}\left((u^2 - v^2)\cos 2\theta + 2uv\sin 2\theta\right)n_+. \end{aligned}$$

To specify the conics precisely, let us show the way of parameter extraction for the conics in GAC.

1.6.2 Parameter extraction

It is well known that the type of a given unknown conic can be read off its matrix representation, which in our case for a conic is given by

$$Q = \begin{pmatrix} -\frac{1}{2}(\bar{v}^+ + \bar{v}^-) & -\frac{1}{2}\bar{v}^\times & \frac{1}{2}v^1 \\ -\frac{1}{2}\bar{v}^\times & -\frac{1}{2}(\bar{v}^+ - \bar{v}^-) & \frac{1}{2}v^2 \\ \frac{1}{2}v^1 & \frac{1}{2}v^2 & -v^+ \end{pmatrix}. \tag{1.9}$$

The entries of (1.9) can be easily computed by means of the inner product:

$$\begin{aligned} q_{11} &= Q_I \cdot \tfrac{1}{2}(n_+ + n_-), \\ q_{22} &= Q_I \cdot \tfrac{1}{2}(n_+ - n_-), \\ q_{33} &= Q_I \cdot \bar{n}_+, \\ q_{12} = q_{21} &= Q_I \cdot \tfrac{1}{2}n_\times, \\ q_{13} = q_{31} &= Q_I \cdot \tfrac{1}{2}e_1, \\ q_{23} = q_{32} &= Q_I \cdot \tfrac{1}{2}e_2. \end{aligned}$$

It is also well known how to determine the internal parameters of an unknown conic and its position and the orientation in the plane from the matrix (1.9), [29]. Hence all this can be determined from GAC vector Q_I by means of the inner product.

The parameters of a conic can be obtained from the matrix (1.9) of its IPNS representation, for example:

- center of an ellipse or hyperbola:

$$x_c = \frac{q_{12}q_{23} - 2q_{22}q_{31}}{4q_{11}q_{22} - q_{12}q_{12}}, \quad y_c = \frac{q_{31}q_{21} - 2q_{11}q_{32}}{4q_{11}q_{22} - q_{12}q_{12}}, \tag{1.10}$$

- semiaxis of an ellipse:

$$a, b = \frac{\sqrt{(2A(q_{11} + q_{22} \pm \sqrt{(q_{11} - q_{22})^2 + q_{12}^2})}}{(4q_{11}q_{22} - q_{12}^2))}, \tag{1.11}$$

  where $A = q_{11}q_{23}^2 + q_{22}q_{13}^2 - q_{12}q_{13}q_{23} + (q_{12}^2 - 4q_{11}q_{22})q_{33}$,

- angle of rotation

$$\theta = \begin{cases} -\arctan \frac{q_{22} - q_{11} - \sqrt{(q_{11} - q_{22})^2 + q_{12}^2}}{q_{12}}, & q_{12} \neq 0 \\ 0, & q_{12} = 0, \quad q_{11} < q_{22} \\ \frac{\pi}{2}, & q_{12} = 0, \quad q_{11} > q_{22} \end{cases} \tag{1.12}$$

Other parameters can be derived with the help of eigenvalues of the quadratic form matrix. For more details see [30].

1.6.3 Transformations

The main advantage of GAC compared to other models (for instance, $\mathbb{G}_6$) is that it is fully operational in the sense that it allows all Euclidean transformations, ie., rotations and translations. But not just that, it also allows scaling in the sense of (1.4). Hence, like in the case of CGA (or $\mathbb{G}_{3,1}$), one obtains all conformal transformations: rotation, translation and scaling.

Example 2. Let us consider the IPNS representation of the axis-aligned ellipse with the semi-axes $a = 2$, $b = 4$ centred in $(u, v) = (0, 2)$:

$$E = 0.8e_2 - 0.5e_3 - 0.3e_4 + 0.5e_6 + 0.3e_7.$$

The rotor for a rotation around the origin by the angle $\frac{\pi}{3}$ is given by $R = R_+(R_1 \wedge R_2)$, where

$$R_+ = \cos(\tfrac{\pi}{6}) + \sin(\tfrac{\pi}{6})e_1 \wedge e_2 = \tfrac{\sqrt{3}}{2} + \tfrac{1}{2}e_1 \wedge e_2, \tag{1.13}$$

$$R_1 = \cos(\tfrac{\pi}{3}) + \sin(\tfrac{\pi}{3})\bar{n}_\times \wedge n_- = \tfrac{1}{2} + \tfrac{\sqrt{3}}{2}\bar{n}_\times \wedge n_-, \tag{1.14}$$

$$R_2 = \cos(\tfrac{\pi}{3}) - \sin(\tfrac{\pi}{3})\bar{n}_- \wedge n_\times = \tfrac{1}{2} - \tfrac{\sqrt{3}}{2}\bar{n}_- \wedge n_\times. \tag{1.15}$$

Rotated ellipse has equation:

$$E_{rotated} = -0.69282e_1+0.4e_2-0.5e_3+0.15e_4-0.25981e_5+0.5e_6-0.15e_7+0.25981e_8$$

The scalor for a by $\alpha \in \mathbb{R}^+$ is given by $S = S_+S_-S_\times$, where

$$S_+ = \frac{\alpha+1}{2\sqrt{\alpha}} + \frac{\alpha-1}{2\sqrt{\alpha}}\bar{n}_+ \wedge n_+, \tag{1.16}$$

$$S_- = \frac{\alpha+1}{2\sqrt{\alpha}} + \frac{\alpha-1}{2\sqrt{\alpha}}\bar{n}_- \wedge n_-, \tag{1.17}$$

$$S_\times = \frac{\alpha+1}{2\sqrt{\alpha}} + \frac{\alpha-1}{2\sqrt{\alpha}}\bar{n}_\times \wedge n_\times. \tag{1.18}$$

For more information see [16].

Consider axis-aligned ellipse with the semi-axes $a = 2, b = 4$ centred in $(u, v) = (0, 2)$.

The result of applying the scaling by 2 is the ellipse

$$E_{scaled} = 3.2e_2 - 1.0e_3 - 0.6e_4 + 1.0e_6 + 0.6e_7$$

and translations by vectors $(0, 2), (2, 0), (-3, 2)$ are:

$$E(0,2) = 2.76923e_1 + 1.23077e_2 + 0.73077e_3 - 0.19231e_4 + 1.73077e_6 + 0.19231e_7,$$

$$E(2,0) = 2.46154e_2 + 1.65385e_3 - 0.19231e_4 + 2.65385e_6 + 0.19231e_7,$$

$$E(-3,2) = -4.15385e_1 + 2.96154e_3 - 0.19231e_4 + 3.96154e_6 + 0.19231e_7,$$

respectively. All transformations are shown in Figure 1.3.

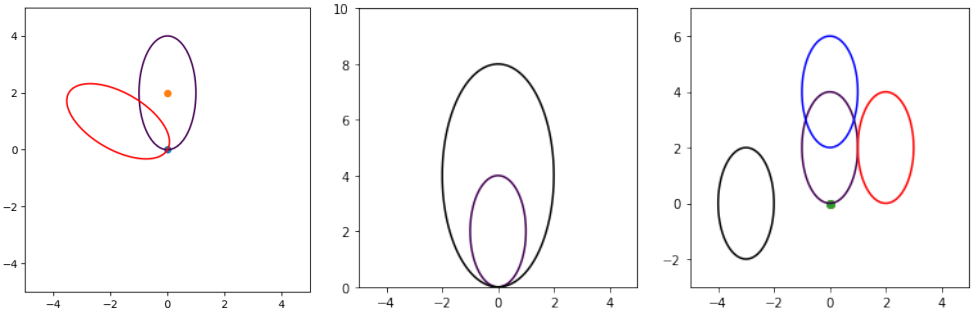

Figure 1.3: Transformations

1.6.4 Intersections and contact points in GAC

In this section we provide a procedure for intersecting two conics, particularly ellipses with common centre in the coordinate origin but in a general mutual position otherwise. Moreover, we consider a system of circumscribed ellipses as in Figure 1.7 and show a procedure for detecting the first order contact points, ie., points where the ellipses touch with identical first order derivative. Again, the contribution of GAC lies in avoiding the use of a solver which leads to accuracy improvement.

Let us first describe some differences to CRA or its 3–dimensional version CGA (Conformal Geometric Algebra). Crucial difference lies in the type of objects that are intrinsic to respective structures. For CRA (CGA), spheres (circles) are the geometric primitives that may be represented by specific elements. Taking into account that lines and planes are spheres with infinite radii and a point pair is a 1–dimensional sphere, we receive all geometric primitives for analytic geometry. Moreover, intersection still remain such objects, indeed, an intersection of two spheres or two circles are circles or point pairs, respectively. Therefore, intersections that are realised by wedge of IPNS representations remain representatives of Euclidean primitives intrinsic to CRA (CGA). On contrary, in GAC the situation is different. Even if we restrict to the case of co–centric ellipses, their intersection is a "four point" which has no meaning in the sense of conic–sections. Indeed, a planar conic is generated by five points at least. This leads to an algorithm that may be used for co–centric conics (all types). On the other hand, the algorithm is still geometric–based and may be realised by a sequence of simple operations in GAC, ie., there is no numerical solver involved.

Intersections

Let us now present the procedure for getting intersections of two co–centric ellipses, ie., the set up according to Figure 1.4. Note that we may assume, without loss of generality, that the ellipses have four points of intersections. Other cases are not of our interest and would be recognized by the form of GAC element representing the pair of intersecting lines depicted in Figure 1.4 as an imaginary or degenerate conic. Furthermore we may assume that the ellipse centres are situated at the coordinate origin, otherwise the whole picture may be translated in GAC to fulfil this assumption. More information can be found in [31].

We start by taking two IPNS representations of ellipses E_1 and E_2 and wedging them. The result corresponds to the common points of both geometric primitives.

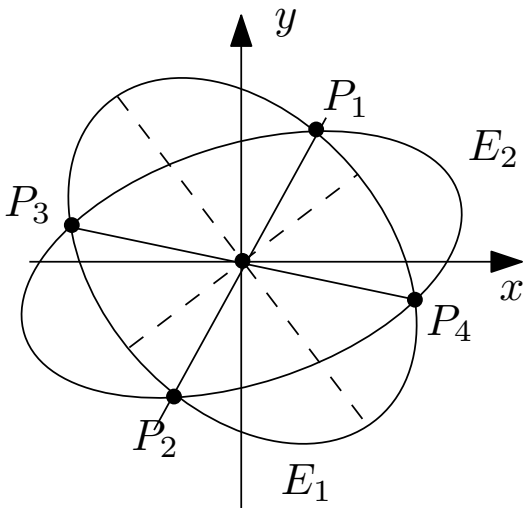

Figure 1.4: Initial setting of the intersection problem

This is standard operation intrinsic to any geometric algebra. In our case, we receive an IPNS representative of a four–point $E_1 \wedge E_2 = P_1 \wedge P_2 \wedge P_3 \wedge P_4$ as in Figure 1.4. Let us recall that this does not represent any geometric entity intrinsic to GAC.

Therefore, as the next step, we construct a degenerate conic, more precisely a pair of intersecting lines $(E_1 \wedge E_2)^* \wedge \overline{n}_+$, where $\overline{n}_+$ represents origin of the Euclidean coordinates and therefore the common ellipse centre, and $(E_1 \wedge E_2)^*$ is the four–point's OPNS representation.

Now we need to decompose the pair of lines to two single lines. First, we construct the matrix Q of its quadratic form by (1.9). Note that Q is a symmetric singular matrix. To decompose a degenerate conic we follow an algorithm described in [32]. We recall the algorithm just to present that all operations involved are sums and products in the form of determinant calculations. The only numerical inaccuracy may be imported by a square root calculation.

Indeed, to decompose a pair of intersecting lines into two distinct lines we have to find a skew-symmetric matrix P formed by parameters λ, μ, and τ such that $N = Q + P$ is of rank 1. Thus in our case we have to find the parameters λ, μ, and τ such that the following matrix sum has rank 1:

$$\begin{pmatrix} q_{11} & q_{12} & q_{13} \\ q_{21} & q_{22} & q_{23} \\ q_{31} & q_{32} & q_{33} \end{pmatrix} + \begin{pmatrix} 0 & \tau & -\mu \\ -\tau & 0 & -\lambda \\ \mu & \lambda & 0 \end{pmatrix}. \tag{1.19}$$

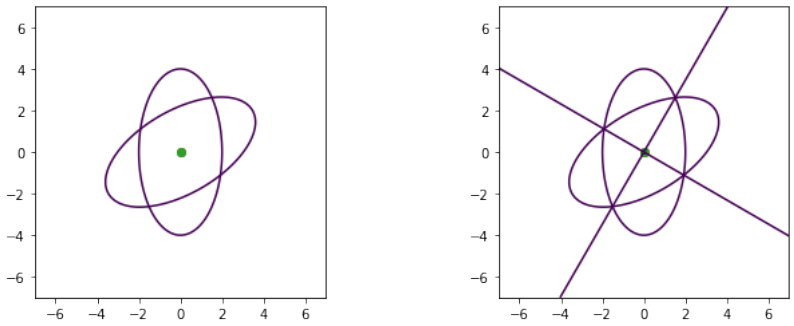

(a) Ellipse setting (b) Pair of lines

Figure 1.5: Setting of Example 3

The rank condition reads that every 2×2 submatrix determinant must vanish. Thus the necessary conditions for the parameters λ, μ, and τ are:

$$\tau^2 = -\begin{vmatrix} q_{11} & q_{12} \\ q_{21} & q_{22} \end{vmatrix}, \quad \mu^2 = -\begin{vmatrix} q_{11} & q_{13} \\ q_{31} & q_{33} \end{vmatrix}, \quad \lambda^2 = -\begin{vmatrix} q_{22} & q_{23} \\ q_{32} & q_{33} \end{vmatrix}$$

This determines the parameters λ, τ, and μ up to their sign. In general case, to get precise values of λ, μ, and τ, one can take a non–zero column of the matrix dual to Q and divide it with a specific factor, see [32]. In the case that the lines are passing through the origin, the division may be omitted and thus only the dual matrix, ie., nine determinants of order 2, have to be calculated, see [32].

By taking an arbitrary nonzero row and a nonzero column in the matrix N we get the coefficients of the respective separated lines. We shall now recall that a single line represents no conic and therefore it is not a geometric primitive intrinsic to GAC. Yet it is understood as an element of subalgebra CRA, ie., a model of 2–dimensional Euclidean space formed by a Clifford algebra $\mathcal{C}l(3,1)$, see [26].

Example 3. To construct an ellipse, we need the semi–axes lengths a, b, centre coordinates c_1, c_2 and the angle of rotation θ, (1.7). Let us consider two ellipses $Ell1$ and $Ell2$ with parameters $(a, b, c_1, c_2, \theta) = (2, 4, 0, 0, 0)$ and $(4, 2, 0, 0, \frac{\pi}{6})$, respectively. Their IPNS representations will then be of the form

$$Ell1 = \bar{n}_+ + \frac{3}{5}\bar{n}_- - \frac{16}{5}n_+$$

and

$$Ell2 = \bar{n}_+ - \frac{3}{10}\bar{n}_- - \frac{3\sqrt{3}}{10}\bar{n}_\times - \frac{16}{5}n_+.$$

If transformed to OPNS, it becomes four-vector, therefore it is clear that it corresponds to a wedge of four GAC points. By wedging the origin represented by $\bar{n}_+$, we receive an OPNS representation of a degenerated conic, more precisely of a pair of intersecting lines. Their IPNS form is

$$-\frac{72}{25}\bar{n}_- - \frac{24\sqrt{3}}{25}\bar{n}_\times.$$

The type of the conic may be easily checked using their matrix form

$$\begin{pmatrix} \frac{36}{25} & \frac{12\sqrt{3}}{25} & 0 \\ \frac{12\sqrt{3}}{25} & -\frac{36}{25} & 0 \\ 0 & 0 & 0 \end{pmatrix}.$$

After normalization, equation of this conic is $x^2 - y^2 + \frac{24\sqrt{3}}{3}xy = 0$. Thus we have a pair of lines containing all four ellipses' intersections and the origin, see Figure 1.5b.

Let us provide all necessary inputs for procedure of line separation (1.19) in the same form:

$$\begin{pmatrix} \frac{36}{25} & \frac{12\sqrt{3}}{25} & 0 \\ \frac{12\sqrt{3}}{25} & -\frac{36}{25} & 0 \\ 0 & 0 & 0 \end{pmatrix} + \begin{pmatrix} 0 & -\frac{12\sqrt{3}}{25} & 0 \\ \frac{36\sqrt{3}}{25} & -\frac{36}{25} & 0 \\ 0 & 0 & 0 \end{pmatrix},$$

i.e. $\mu = 0, \quad \tau = -\frac{24\sqrt{3}}{25}, \quad \lambda = 0$. Therefore the pair of lines' matrix is of the form

$$\begin{pmatrix} \frac{36}{25} & -\frac{12\sqrt{3}}{25} & 0 \\ \frac{36\sqrt{3}}{25} & -\frac{36}{25} & 0 \\ 0 & 0 & 0 \end{pmatrix}$$

and thus the form of a separated lines may be easily derived according to the first (non–zero) row and column. After normalization we receive

$$\frac{1}{2}x + \frac{\sqrt{3}}{2}y = 0, \quad \text{and} \quad \frac{\sqrt{3}}{2}x - \frac{1}{2}y = 0.$$

It is clear that they are perpendicular which has been expected due to symmetries.

Thus we get a system of quadratic (Ellipse) and linear (Line) equations, which is reduced to the one quadratic equation, that does not require the use of the solver. In our case

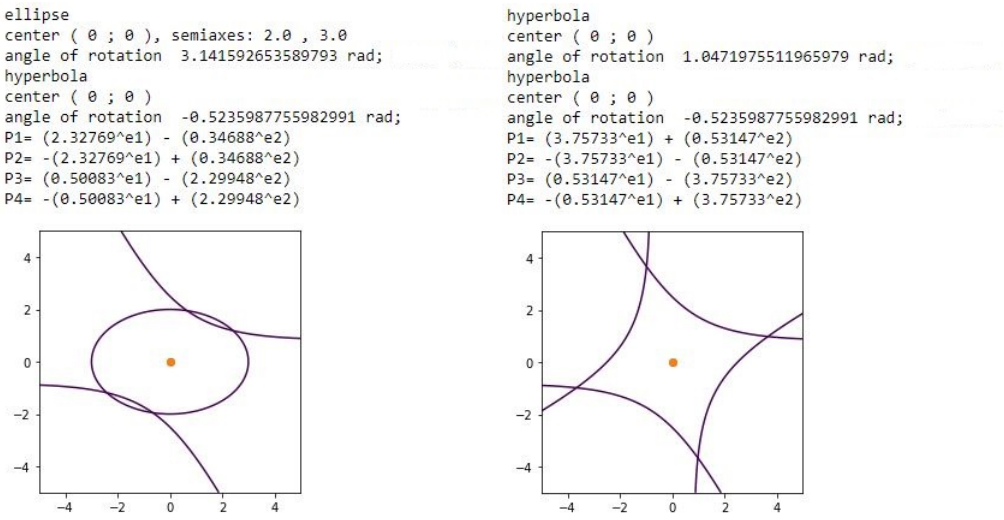

(a) Ellipse and Hyperbola (b) Hyperbola and Hyperbola

Figure 1.6: Non-degenerate centralized conics

$$\begin{cases} x + \sqrt{3}y = 0, \\ \frac{x^2}{4} + \frac{y^2}{16} = 1, \end{cases}$$

for $x = -\sqrt{3}y$, we get $13y^2 - 16 = 0$ and $y = \pm\frac{4\sqrt{13}}{13}$, $x = \mp\frac{4\sqrt{39}}{13}$. So we get intersection points $[\frac{4\sqrt{39}}{13}, -\frac{4\sqrt{13}}{13}]$ and $[-\frac{4\sqrt{39}}{13}, \frac{4\sqrt{13}}{13}]$. The same way by using the line $x + \sqrt{3}y = 0$ we get the following points: $[\frac{4\sqrt{39}}{13}, \frac{4\sqrt{13}}{13}]$ and $[-\frac{4\sqrt{39}}{13}, -\frac{4\sqrt{13}}{13}]$.

The described procedure can be applied to different types of the co–centred conics with 4 intersection points.

Example 4. Figure 1.6 demonstrates the output of the Python code for different types of the co–centred conics with 4 intersection points. It shows that our considerations are valid not only for ellipses but for an arbitrary pair of non-degenerate centralized conics, see [33] for proofs.

Example 5. In the case of axes aligned ellipses we can apply a more geometric approach, [28]. Given two ellipses $Ell1$ and $Ell2$ with parameters $(a, b, c_1, c_2, \theta) = (2, 4, 0, 0, 0)$ and $(4, 2, 0, 0, 0)$, respectively, we determine their IPNS representations according to (1.7) in the form

$$Ell1 = \bar{n}_+ + \frac{3}{5}\bar{n}_- - \frac{16}{5}n_+$$

and

$$Ell1 = \bar{n}_+ - \frac{3}{5}\bar{n}_- - \frac{16}{5}n_+,$$

the intersecting points form a circle C that may be constructed by $(Ell1 \wedge Ell2)^* \wedge \bar{n}_+$, [28], and thus represented by an element

$$C = \frac{6}{5}\bar{n}_+ - \frac{96}{5}n_+,$$

ie., its equation will be

$$x^2 + y^2 - \frac{32}{5} = 0.$$

Then we can construct a pair of intersecting lines $(Ell1 \wedge Ell2)^* \wedge \bar{n}_+$ with IPNS representation

$$\frac{6}{5}\bar{n}_- - \frac{96}{25}n_+,$$

ie., of the equation (after normalization) $-x^2 + y^2 = 0$.

The line decomposition procedure, although not necessary in this particular case, will lead to a pair of lines $y = x$ and $y = -x$. As CRA elements they are of the form $l_1 = -\frac{\sqrt{2}}{2}e_1 + \frac{\sqrt{2}}{2}e_2$ and $l_2 = \frac{\sqrt{2}}{2}e_1 + \frac{\sqrt{2}}{2}e_2$, respectively. Then it is enough to calculate the intersection $C \wedge l_1$ and $C \wedge l_2$ to get two point pairs P_1, P_2 in CRA. Consequently, a procedure for a point pair decomposition must be applied in the form

$$p_{i1} = \frac{-\sqrt{P_i \cdot P_i} + P_i}{n_+ \cdot P_i}, \quad p_{i2} = \frac{\sqrt{P_i \cdot P_i} + P_i}{n_+ \cdot P_i} \quad \text{for} \quad i = 1, 2.$$

In this very simple case we receive CRA points

$$\bar{n}_+ \pm \frac{4\sqrt{5}}{5}e_1 \pm \frac{4\sqrt{5}}{5}e_2 + \frac{16}{5}n^+,$$

which means that the points of intersections are of the form $[\pm\frac{4\sqrt{5}}{5}, \pm\frac{4\sqrt{5}}{5}]$.

Contact points

As mentioned above, by a contact points we understand first order contact points, ie., points where two curves have identical first order derivative. We shall describe how to receive a set of contact points for a given system of co–centred ellipses.

Such system is formed as in Figure 1.7 beginning with two intersecting ellipses E_1 and E_2. Then an ellipse E_2' is constructed from E_2 just by scaling in such a way that E_2' is circumscribed to E_1, ie., they have two contact points. Then an ellipse E_1' would be constructed from E_1 such that it would be circumscribed to E_2' etc.

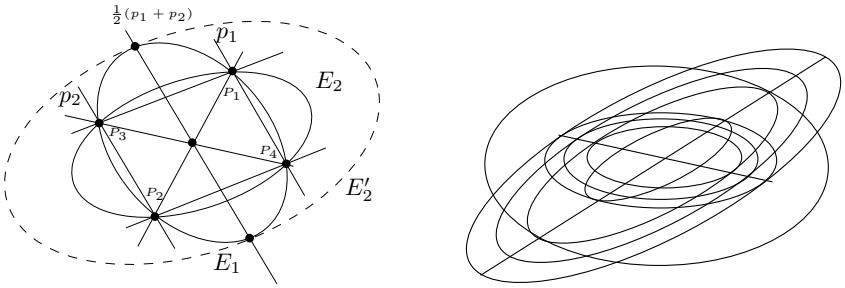

Figure 1.7: Initial setting of contact points problem

Proposition 1.6.3. Given a system of co–centric ellipses as in Figure 1.7, the contact points form a pair of intersecting lines. Furthermore, one of these lines is the axis of lines p_1 and p_2 denoted in Figure 1.7 as $\frac{1}{2}(p_1 + p_2)$ and, similarly, the other line is the axis of the lines p_3 and p_4 in Figure 1.7.

Taking into account that the ellipses are co–centric and their symmetry properties, it is obvious that 4 points of their intersection form a parallelogram with diagonals passing through the common centre. The line $\frac{1}{2}(p_1 + p_2)$ is the middle line of the parallelogram and passes through the common centre S of the ellipses. Note that the notation $\frac{1}{2}(p_1 + p_2)$ for the axis of p_1 and p_2 is the way to calculate this line in CRA. Indeed, this is true for IPNS representations of p_1 and p_2.

Proposition 1.6.4. Given a system of co–centric ellipses as in Figure 1.7, a scalor transforming an ellipse E_2 to E_2' may be calculated as $SP = \frac{|SK'|}{|SK|}$, where K and K' are the intersection points of the ellipses E_2 and E_1 with the line $\frac{1}{2}(p_1 + p_2)$ and S is the common centre of the ellipses.

Due to the fact that K' is the contact point of ellipses E_2' and E_1, scaling ellipse E_2 until the contact with E_1 means scaling the length section SK up to the length of SK', therefore $SP = \frac{|SK'|}{|SK|}$.

Remark. The transformation of E_2 to E_2' is then given in GAC by a scalor according to 1.16. In the case of centralized ellipses with the centre in the coordinate system origin we may just multiply the semi–axes lengths by the scaling factor.

1.7 QC2GA

Let us recall another construction of a conformal model for conic sections in a Euclidean space. Quadric Conformal Geometric Algebra (QCGA) is a conformal model for representation of quadratic surfaces (quadrics) in three dimensional Euclidean space. Its two–dimensional version, QC2GA, then contains conics as objects, [34].

More precisely, QCGA $\mathbb{G}_{9,6}$ is defined over a 15-dimensional vector space. The base vectors of the space $\mathbb{R}^{9,6}$ are divided into three groups of the Euclidean vectors, "origins" and "infinities", respectively. In [34], the authors denote these respective groups as $\{e_1, e_2, e_3\}$, $\{e_{O_1}, e_{O_2}, e_{O_3}, e_{O_4}, e_{O_5}, e_{O_6}\}$, and $\{e_{\infty_1}, e_{\infty_2}, e_{\infty_3}, e_{\infty_4}, e_{\infty_5}, e_{\infty_6}\}$.

Consequently, subalgebra $\mathbb{G}_{5,3}$ of $\mathbb{G}_{9,6}$, ie., QC2GA, is isomorphic to GAC (Geometric Algebra for Conics), more precisely they are the same algebras with different bases. The basis transformation is given by:

$$\begin{aligned} \bar{n_+} &= e_{O_1} + e_{O_2}, \quad n_+ = \frac{e_{\infty_1} + e_{\infty_2}}{2}, \\ \bar{n_-} &= e_{O_1} - e_{O_2}, \quad n_+ = \frac{e_{\infty_1} - e_{\infty_2}}{2}, \\ \bar{n_\times} &= e_{O_3}, \quad n_\times = e_{\infty_3}. \end{aligned}$$

Such a basis change has benefit in easier representation of translator, yet other transformations are then more complicated. Therefore, we will work in GAC in this thesis.

1.8 Summary of Chapter 1

Geometric Algebra (GA) offers a powerful mathematical framework for handling geometric operations with elegance and efficiency. Originating from Grassmann algebras and Clifford algebras, GA unifies geometric primitives and transformations within a single algebraic structure, providing a seamless approach to geometric analysis and manipulation.

Throughout this chapter, we have explored the fundamental concepts of Grassmann algebras and Clifford algebras, highlighting their role in forming the basis of Geometric Algebra. One of the key features of GA is its ability to represent geometric entities such as points, lines, planes, and volumes using multivectors, which are elements of a geometric algebra. These multivectors capture not only

the geometry of objects but also their spatial relationships and transformations. Through the use of the outer, inner, and geometric product operations, GA enables the manipulation and analysis of these geometric entities in a rigorous and intuitive manner.

Chapter 2

Switched systems

2.1 Dynamical system

By dynamical system we mean the triplet $(\mathbb{R}, \mathbb{R}^n, f)$, where $\mathbb{R}^n$ is a metric space, which we call phase or state space, and $f(t, \cdot)$ is a system of evolution operators defined as the mapping $f(t, \cdot) : \mathbb{R}^n \to \mathbb{R}^n$, which maps the initial state $x(0) \in \mathbb{R}^n$ to some state $x(t) \in \mathbb{R}^n$.

Dynamical system can be generated by a form of the system of Ordinary Differential Equations (ODE)

$$\dot{\boldsymbol{x}} = \boldsymbol{f}(t, \boldsymbol{x}), \tag{2.1}$$

in which a function $\boldsymbol{f} \in C(\mathbb{R}^{n+1}, \mathbb{R}^n)$ describes the time dependence of a point $\boldsymbol{x} \in \boldsymbol{X}$ and the derivative is considered w.r.t. time.

Definition 2.1.1. Suppose that $\boldsymbol{f} \in C(\mathbb{R}^{n+1}, \mathbb{R}^n)$. Then $\boldsymbol{x}$ is a solution of the differential equation (2.1) on the interval $I \subseteq \mathbb{R}^n$ if $\boldsymbol{x}(t)$ is differentiable on I and if for all $t \in I$, $\boldsymbol{x}(t) \in \mathbb{R}^n$ and $\dot{\boldsymbol{x}} = \boldsymbol{f}(t, \boldsymbol{x}(t))$.

Given a differential equation with $\boldsymbol{f} \in C(\mathbb{R}^n)$, the solution $\phi(t, \boldsymbol{x_0})$ of the initial value problem

$$\dot{\boldsymbol{x}} = \boldsymbol{f}(t, \boldsymbol{x}), \quad \boldsymbol{x}(0) = \boldsymbol{x}_0 \tag{2.2}$$

with $\boldsymbol{x_0} \in \mathbb{R}^n$ is dynamical system on $\mathbb{R}^n$ if and only if for all $\boldsymbol{x}_0 \in \mathbb{R}^n$, $\phi(t, \boldsymbol{x}_0)$ is defined for all $t \in \mathbb{R}$.

In our case it describes a mechanical system, which is characterized by its position and behaviour, while the motion law describes the rate of change of the state of the system.

In the simplest case the law of motion is described as an autonomous system of ordinary differential equations:

$$\dot{x}_i = f_i(x_1, x_2, \ldots, x_m), \quad i = 1, \ldots m, \tag{2.3}$$

where $f_i \in C(\mathbb{R}^m) = C(\mathbb{R}^m, \mathbb{R}^m)$.

If the variables $(x_1, x_2, \ldots, x_m) \in \mathbb{R}^m$, where $x_i = x_i(t)$ are considered as coordinates of a point $\boldsymbol{x}$ in an m-dimensional space, then the corresponding state of the dynamical system may be determined by this point $\boldsymbol{x}$ and the differential equations (2.3) may be rewritten as

$$\dot{\boldsymbol{x}}(t) = \boldsymbol{f}(\boldsymbol{x}).$$

When searching for the solution of the system, generated by system of autonomous ODEs, its existence and uniqueness should be guaranteed. Indeed if in the following we are given a set of respective initial conditions, we have to be sure that it each point the solution exists and is unique. Therefore, let us recall the theorem of existence and uniqueness for the solution of the differential equation.

Theorem 2.1.1. ([35]) Let E be an open subset of $\mathbb{R}^n$ containing $\boldsymbol{x}_0$, assume that $\boldsymbol{f} \in C^1(E)$. Then there exists an $a > 0$ such that the initial value problem

$$\dot{\boldsymbol{x}}(t) = \boldsymbol{f}(\boldsymbol{x}), \quad x(0) = x_0 \tag{2.4}$$

has a unique solution $\boldsymbol{x}$ on the interval $[-a; a]$. In addition, for each point $\boldsymbol{x_0} \in E$ there is a maximal interval $J = (\alpha; \beta)$: if (2.4) has solution $\boldsymbol{y}$ on the interval I then $I \subseteq J$ and $\boldsymbol{y}(t) = \boldsymbol{x}(t)$ for all $t \in I$.

Let us now recall the basic definitions of trajectory, phase portrait and equilibrium.

Definition 2.1.2 ([36])**.** A trajectory of the dynamical system (2.2) is the set of points in state space $\mathbb{R}^n$ that are the future states resulting from a given initial state $\boldsymbol{x}(0)$.

Definition 2.1.3. A phase portrait of the system (2.2) is a plot of multiple phase curves corresponding to different initial conditions $\boldsymbol{x}(0)$ in the same phase plane.

Definition 2.1.4. An equilibrium (or equilibrium point) of a dynamical system (2.3), generated by an autonomous system of ordinary differential equations (ODEs) is a solution of (2.3) that does not change with respect to time t.

Based on the type of the state, dynamical systems are classified into:

- Continuous, if $(x_1, x_2, \dots, x_m) \in \mathbb{R}^m, \quad m \geq 1$. In a continuous dynamical system, a trajectory is a curve in the state space;

- Discrete, if the set of achievable states $\{q_1, q_2, \dots\}$ is countable. In a discrete dynamical system, a trajectory is a set of isolated points in the state space;

- Hybrid, if one of the state takes values in $\mathbb{R}^l$ while the other part takes values in a finite set,i.e if there exists $0 < l < m$ such that $(x_1, x_2, \dots, x_l) \in \mathbb{R}^l$, and $(x_{l+1}, x_2, \dots, x_m) \in \{q_1, q_2, \dots, \quad q_k\}$, [37].

2.2 Basic theory of switched systems

Now let us recall the basic terminology in the switched systems theory.

Definition 2.2.1. Switched system is the system of differential equations in the vector form of the type

$$\dot{\boldsymbol{x}} = \boldsymbol{f}_{\sigma(t)}(\boldsymbol{x}); \tag{2.5}$$

where $\boldsymbol{x} = (x_1, \dots, x_m) \in \mathbb{R}^m$ is called *a continuous state*, $\sigma : \mathbb{R} \to \mathbb{R}$ is a left continuous piecewise constant function of time with finite amount of pieces, that is called *a discrete state*(switching signal) with values from an index set $M := \{1, \dots, n\}$, and $f_{\sigma(t)} : \mathbb{R}^m \to M$ is a family of functions of class C^k for sufficiently large k.

Along with (2.5) we consider the initial condition $\boldsymbol{x}(0) = \boldsymbol{x}_0$, $\boldsymbol{x}_0 \in \mathbb{R}^m$,

Definition 2.2.2. Let $\boldsymbol{x}$ be a continuous and piecewise differentiable function on $\mathbb{R}$. Then $\boldsymbol{x}$ is a solution of the switched system (2.5) on $\mathbb{R}$ if for all $t \in \mathbb{R}, \quad \boldsymbol{x}(t) \in \mathbb{R}^n$ and $\dot{\boldsymbol{x}} = \boldsymbol{f}_{\sigma(t)}(\boldsymbol{x}(t))$, and at the breakpoints, sigma has the right side derivative.

The form of the right hand side of the dynamical system is described by the switching signal. Namely, at specific time moments, ie., for $t = \tau_1, \dots, \tau_l$, the system changes its form from $\sigma(\tau_i)$ to $\sigma(\tau_{i+1})$, hence the trajectory of the system, starting at the time $t = \tau_i$, is given by the vector field $\boldsymbol{f}_{\sigma(\tau_{i+1})}$ instead of $\boldsymbol{f}_{\sigma(\tau_i)}$. In the works on switched systems, switching times are usually random or are given by some law. In the sequel, we consider a different formulation of the problem, ie., the switching signal is under our control, meaning that we are changing the behaviour of the system.

Definition 2.2.3. We say that the switched system

$$\dot{\boldsymbol{x}} = \boldsymbol{f}_{\sigma(t)}(\boldsymbol{x})$$

is *controllable* if for any two points $A, B \in \mathbb{R}^m$ from the state space there exists a switching signal generating a trajectory from A to B.

Remark. The above definition corresponds to the concept of controllability for a control system of the form

$$\dot{\boldsymbol{x}} = f(\boldsymbol{x}, \boldsymbol{u}) \tag{2.6}$$

where the control $\boldsymbol{u}$ plays the role of a switching signal.

As a special case of the system (2.5), we recall the linear switched systems, [4], of the form

$$\dot{\boldsymbol{x}} = A_{\sigma(t)}\boldsymbol{x}, \tag{2.7}$$

where $A_{\sigma(t)} \in \mathcal{M}at_2, \quad \sigma(t) \in \{1 \dots n\}$ are given matrices. It is a linear system of ODEs with piecewise constant matrix function and thus, we have a unique solution for any initial value problem for (2.6) and its extendability on the whole real line. The solution of the switched system is a combination of the solutions of the particular subsystems on the corresponding interval.

Depending on the type of switch the following types of switched systems are distinguished [10]:

- State-dependent versus time-dependent;
- Autonomous (no direct control over the switching mechanism that triggers the discrete events) versus controllable (direct control over the switching mechanism)

Stability issue of linear systems

In the study of stability of (2.6), we asssume that σ has infinitely many discontinuities $\tau_1 < \tau_2 < \dots$. Particular interest in the study of switched systems is the study of the relationship between the stability of each subsystem and the switched system (2.7).

Since the switched system (2.6) is a linear system of ODEs with a piecewise constant matrix function $A_{\sigma(\cdot)}$, we use the standard concept of Lyapunov stability of solutions.

In the general case with an arbitrary switching signal, the stability of the switched system can not be guaranteed by the stability of each subsystem. For example, a 2×2 linear switched system with two stable subsystems with matrices

$$A_1 = \begin{pmatrix} 0 & 1 \\ -2 & 0 \end{pmatrix}, \quad A_2 = \begin{pmatrix} 0 & 1 \\ -\frac{1}{2} & 0 \end{pmatrix}$$

is stable if σ is such that the solution of (2.6) is a combination of solutions of subsystems, such that solutions of the first subsystem goes through the first and third quadrants, and the solutions of the second subsystem goes through the second and fourth quadrants. In this case all trajectories approach zero for $t \to \infty$, [3]. Simultaneously, the switched system is not stable if σ is such that the solution of 2.7 is a combination of solutions of subsystems such that solutions of the first subsystem goes through the second and fourth quadrants, and the solutions of the second subsystem goes through the first and third quadrants, see Figure 2.1.

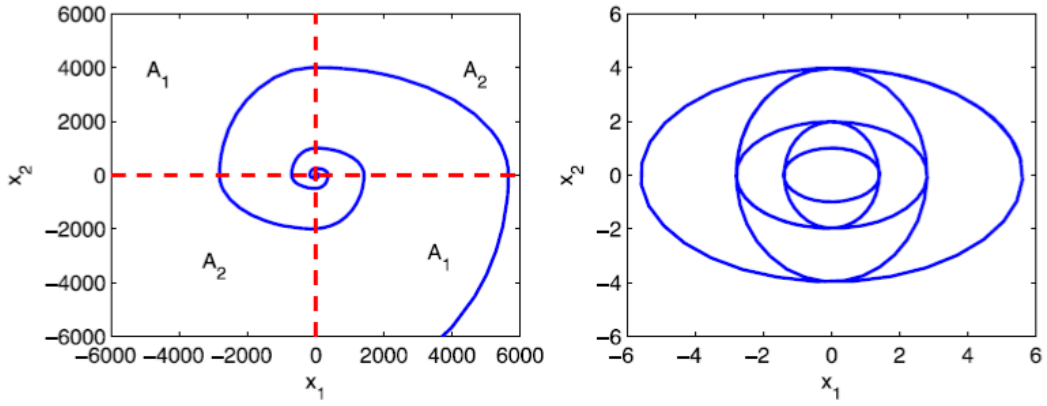

Figure 2.1: Unstable switched system with stable subsystems ([4])

However, our interest is not directed to stability, but to the controllability of switched systems.

The main goal of the following chapter is to consider the standard approach to finding the phase portrait for each subsystem of the 2×2 switched system.

2.3 Standard methods

Let us now concentrate on one of the subsystems of the switched system. Various methods of studying these systems include using eigenvalues, phase portrait,

nullclines etc. Let us consider some of them more precisely.

2.3.1 Nullclines

Consider a system of differential equations of the form

$$\frac{dx}{dt} = f(x,y), \quad \frac{dy}{dt} = g(x,y).$$

For our goals it is sufficient to have the existence and uniqueness of the local solution. Therefore it is enough to request f and g to be continuously differentiable functions in $\mathbb{R}^m$. That guarantees the local existence of the solution, see theorem 2.1.1. The trajectory of solutions in the phase space is given by the functions f and g as follows: here $f(x,y)$ determines the motion in the x direction at position (x,y) and $g(x,y)$ determines the motion in the y direction at position (x,y). A nullcline is a curve in the phase space where the vector field is defined by the differential equation points in a particular direction.

There are two special cases:

- x-nullcline, ie., the set of points in the phase plane where $\frac{dx}{dt} = 0$. This corresponds to the points (x,y) such that $f(x,y) = 0$. y-motions are further referred as vertical.
- y-nullcline, ie., the set of points in the phase plane where $\frac{dy}{dt} = 0$. This corresponds to the points (x,y) such that $g(x,y) = 0$. x-motions are further referred as horizontal.

The x-nullcline and y-nullcline divide the phase plane into particular regions. Along the boundary of these regions the solutions are either moving horizontally or vertically. The procedure of construction of the phase portrait is demonstrated on the following example.

Example 6. Consider the system of ordinary differential equations:

$$\frac{dx}{dt} = -x + \frac{y}{2}, \tag{2.8}$$

$$\frac{dy}{dt} = -\frac{x}{2} - y. \tag{2.9}$$

Let us find the nullclines using the condition

$$-x + \frac{y}{2} = 0, \tag{2.10}$$

$$-\frac{x}{2} - y = 0. \tag{2.11}$$

implying that

$$y = 2x, \quad y = -\frac{x}{2}.$$

By substituting (2.10) to (2.9), leading to $\frac{dx}{dt} = 0$, and (2.11) to (2.8), leading to $\frac{dy}{dt} = 0$, we get that along the nullclines, the vertical motion is described by differential equations

$$\frac{dy}{dt} = -\frac{5y}{4},$$

while the horizontal motion is described by

$$\frac{dx}{dt} = -\frac{5x}{4}.$$

The point $(x, y) = (0, 0)$ must be an equilibrium point, since there is no motion in either x or y directions. Two nullclines are dividing the phase plane into four regions. After checking the signs and directions of nullclines we get the phase portrait, demonstrated in Figure 2.2. For more details, see [35].

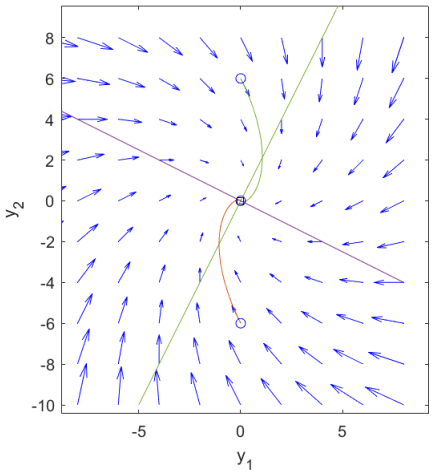

Figure 2.2: Phase plane with nullclines and trajectories

The other approach allows us to get the trajectory directly in terms of the system.

2.3.2 Solution as a parametrized curve

Consider the system of the differential equations of the first order:

$$\begin{cases} \frac{dx}{dt} = f_1(x,y) \\ \frac{dy}{dt} = f_2(x,y) \end{cases}. \tag{2.12}$$

In our case, the existence and uniqueness of a local solution suffices; therefore, it suffices to impose the continuously differentiability condition on the functions $f_1(x,y)$ and $f_2(x,y)$, see 2.1.1. The trajectory is parametrized as $\Gamma = \begin{cases} x = u_1(t) \\ y = u_2(t) \end{cases}$, where (u_1, u_2) is a solution of (2.12) on the interval (a,b). Then we have

$$f_2(u_1(t), u_2(t))u_1'(t) - f_1(u_1(t), u_2(t))u_2'(t) = 0,$$

for $t \in (a,b)$. Now let us consider $(f_2(u_1(t), u_2(t)), -f_1(u_1(t), u_2(t)))$ and $(u_1'(t), u_2'(t))$ as vectors. Then after rewriting in terms of the scalar product, we get:

$$(f_2(u_1(t), u_2(t)), -f_1(u_1(t), u_2(t))) \cdot (u_1'(t), u_2'(t)) = 0$$

for $t \in (a,b)$.

Therefore, we have proved that for any $(x,y) \in \Gamma$, the vector

$$(f_1(x,y), f_2(x,y))$$

is tangent vector of the curve Γ. Now assume that the trajectory Γ is given explicitly as $y = g(x), \quad x \in (a,b)$. Then

$$(f_2(x, g(x)), -f_1(x, g(x)) \cdot (1, g'(x)) = 0$$

for $x \in (\alpha,\beta)$. If, moreover, $f_1(x,y) \neq 0$ for $(x,y) \in \Gamma$, then we get

$$g'(x) = \frac{f_2(x, g(x))}{f_1(x, g(x))}$$

for $x \in (\alpha,\beta)$ and thus, g is a solution of 2.12. Therefore we come to the differential equation

$$\frac{dy}{dx} = y' = \frac{f_2(x,y)}{f_1(x,y)}. \tag{2.13}$$

Consequently, trajectories of (2.12) are integral curves of 2.13.

Let us now consider the types of systems that can occur in 2×2 case.

2.4 Types of 2x2 linear systems depending on equilibrium point

Let us consider a linear homogeneous system with constant coefficients in the form

$$\dot{\boldsymbol{x}} = A\boldsymbol{x}, \quad A = \begin{pmatrix} a & b \\ c & d \end{pmatrix}, \quad a, b, c, d \in \mathbb{R}, \quad A \in \mathcal{M}at_2. \tag{2.14}$$

In the system (2.14), three types of phase trajectories are possible: point, closed curve, unclosed curve. A point on the phase plane corresponds to the equilibrium of the system (2.14), while the closed curve corresponds to the periodic solution, and unclosed to non-periodic solutions of the system (2.14), respectively. The equilibrium points of the system (2.14) can be found by solving the homogenous system: $A\boldsymbol{x} = 0$.

System (2.14) has a unique zero equilibrium position, if $\det A \neq 0$. If $\det A = 0$, then, besides the zero equilibrium position, there are others as well, as in this case, system $Ax = 0$ has an infinite set of solutions. Qualitative behaviour of phase trajectories (type of equilibrium) is determined by the eigenvalues of the system matrix. In the following we consider only the cases $\det A \neq 0$. The eigenvalues of the matrix will be found by solving the characteristic equation

$$\lambda^2 - (a + d)\lambda + ad - bc = 0.$$

Note that $a + d = \mathrm{Tr}A$ (trace of the matrix) and $ad - bc = \det A$, [35]. Classification of equilibrium points in the case when $\det A \neq 0$ is shown in the Table 2.1.

Table 2.1: Classification of equilibrium points in the case $\det A \neq 0$

Roots of characteristic Equation	Point Type
λ_1, λ_2 are real numbers of the same sign $\lambda_1\lambda_2 > 0$	Node
λ_1, λ_2 are real numbers of the opposite sign $\lambda_1\lambda_2 < 0$	Saddle
λ_1, λ_2 are complex numbers $\mathrm{Re}\lambda_1 = \mathrm{Re}\lambda_2 \neq 0$	Focus
λ_1, λ_2 are complex numbers $\mathrm{Re}\lambda_1 = \mathrm{Re}\lambda_2 = 0$	Center

Types of the trajectories are demonstrated on the Poincare diagram, see Figure 2.3.

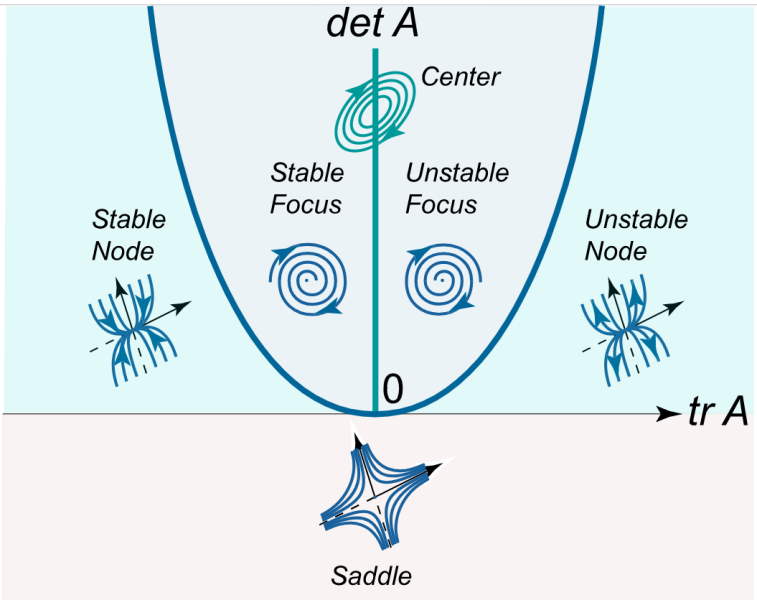

Figure 2.3: Poincare diagram

The stability of equilibrium points can be determined by general theorems on stability (see [8]). So, if the real eigenvalues (or real parts of complex eigenvalues) are negative, then the unique equilibrium point is asymptotically stable. Examples of such equilibrium points are stable node and stable focus.

If $\det A \neq 0$ and the real part of at least one eigenvalue is positive, the corresponding equilibrium point is unstable. For example, it may be a saddle.

Finally, in the case of purely imaginary roots (when the equilibrium point is a center), we are dealing with the classical stability in the sense of Lyapunov.

2.5 Summary of Chapter 2

The Chapter provides an overview of dynamical systems, particularly focusing on the theory of switched systems. In this chapter we introduced controllability of switched systems and presented standard methods for analyzing dynamical systems. Finally, the types of 2x2 linear systems depending on equilibrium points were discussed.

Chapter 3

Control of the switched system by means of GAC

The following chapter deals with the 2×2 switched systems with two subsystems of the special type. More precisely, subsystems have a specific equilibrium point and trajectories intrinsic to Geometric Algebra for Conics. Indeed, the trajectories in question are ellipses and hyperbolas, ie., the elements of GAC.

3.1 Center-Center

In the following section, the case of 2×2 matrices with both subsystems having pure imaginary eigenvalues is studied. Further we will refer to this type of the switched system as Center-Center. This case has already been considered in [38], and the main difference lies in using GAC as a suitable space for geometric operations with the ellipses, for elementary notions see Chapter 1. First, consider one dimensional oscillation problem of a spring pendulum under the condition of absence of external and friction forces and its model equation in the form

$$\ddot{x} = -kx, \quad k \in \mathbb{R} \tag{3.1}$$

with a switchable stiffness coefficient $k > 0$ with two possible values. In the spring pendulum problem, this corresponds to joining and removing an additional spring with stiffness coefficient k_2 to the original spring with stiffness coefficient k_1. Two cases can be considered. If the springs are connected in parallel, the parameter k of the system switches between k_1 and $k_1 + k_2$. If the connection is in series, the parameter k of the system switches between k_1 and $\frac{k_1 k_2}{k_1 + k_2}$.

Let us rewrite the differential equation (3.1) of the pendulum oscillations as a switched system in the form of a system of two differential equations of order one by denoting

$$x_1 = x, \quad x_2 = \dot{x}.$$

Consequently, if we set $\boldsymbol{x} = (x_1, x_2)^T$, the resulting system in the matrix form can be written as

$$\dot{\boldsymbol{x}}(t) = A_i \boldsymbol{x}(t), \quad A_i \in \mathcal{M}at_2(\mathbb{R}), \quad i = 1, 2. \tag{3.2}$$

Without the loss of generality, let us assume that we start and end with the first system $i = 1$. Suppose that two nonzero points (starting $S = [a_1, a_2] \in \mathbb{R}^2$ and end $E = [b_1, b_2] \in \mathbb{R}^2$) are given.

Let us consider the particular type of the switched system (3.2) with the system matrix of the form

$$A_i = \begin{pmatrix} 0 & 1 \\ -\alpha_i & 0 \end{pmatrix}, \quad \alpha_i \in \mathbb{R}^+ \quad \text{for} \quad i = 1, 2.$$

Namely, $\alpha_i \neq 0$. Then the solution of the system is of the form

$$x_1(t) = \gamma_1 \sin(\sqrt{\alpha_1} t) + \gamma_2 \cos(\sqrt{\alpha_1} t),$$
$$x_2(t) = \sqrt{\alpha_1}\gamma_1 \sin(\sqrt{\alpha_1} t) - \sqrt{\alpha_1}\gamma_2 \cos(\sqrt{\alpha_1} t), \quad \gamma_1, \gamma_2 \in \mathbb{R}.$$

The trajectories for the system with pure imaginary eigenvalues are ellipses. In the case $\mathrm{Tr}A_i = 0$, ie., the case of the spring pendulum without damping, for example,

$$A_i = \begin{pmatrix} 0 & 1 \\ -\alpha_i & 0 \end{pmatrix}, \quad \alpha_i \in \mathbb{R}^+,$$

we have an axis-aligned ellipse, while if $\mathrm{Tr}A_i \neq 0$, then the ellipses are rotated and the given switched system is equivalent to the equation describing the oscillatory system with damping. In this case the rotation angle can be calculated from the elements of the conic matrix Q, (1.9), namely of its 2×2 submatrix $\begin{pmatrix} q_{11} & q_{12} \\ q_{21} & q_{22} \end{pmatrix}$ as follows:

$$\theta = \begin{cases} \arctan\left(\frac{1}{q_{12}}\left(q_{22} - q_{11} - \sqrt{(q_{11} - q_{22})^2 + q_{12}}\right)\right), & q_{12} \neq 0 \\ 0, & q_{12} = 0, \quad q_{11} < q_{22} \\ \frac{\pi}{2}, & q_{12} = 0, \quad q_{11} > q_{22} \end{cases}$$

Note that this enables us to solve efficiently even the systems with rotated ellipses as the trajectories.

3.2 Algorithm for a switching path construction

In the following, we describe the algorithm for finding a control of a switched system, ie., finding a path composed of the systems' integral curves from the starting point S to the endpoint E such that the number of switches is minimal. More information ca be found in [31]. Consider the case $n = 2$, ie., only two systems are included, and both starting and final ellipse belong to the same family. To apply the GAC based calculations, it is necessary to get the exact GAC form of the representatives of both families of ellipses. Thus the system of ODEs is solved numerically (e.g. by Runge-Kutta method) with the initial condition at the starting point A. This will give us a set of points representing the initial ellipse. After applying the GAC conic fitting algorithm, [16], we get the ellipse in IPNS representation. Note that according to [33], the algorithm may be further specified by prescribing the resulting ellipse to be axis-aligned and with its centre placed in the origin. This makes the initial trajectories very precise.

1. Get S, E, the starting and final point, respectively, ie., get their conformal embedding $\mathcal{C}(S), \mathcal{C}(E)$ to GAC, (1.2).

2. Find the IPNS representation of the initial ellipse E_1^1 by conic fitting algorithm. Let us denote its semiaxis by a and b.

3. Find the final ellipse E_f in the following two steps:

   - Construct a line l passing through the points $\mathcal{C}([0,0]) = \bar{n}^+$ and $\mathcal{C}(E)$ according to Remark (1.6.1):

     $$l = \mathcal{C}(E) \wedge n_+ \wedge \bar{n}_+ \wedge n_- \wedge n_\times.$$

     Find the intersection point $C = E_1^1 \cap l$ of the line and the starting ellipse, ie., solve a quadratic equation in a Euclidean space as in Example 3.

   - According to Proposition 1.6.4, the scale parameter between the starting and final ellipse is

     $$SP_1 = \frac{|\bar{n}_+ \cdot \mathcal{C}(E)|}{|\bar{n}_+ \cdot \mathcal{C}(C)|}.$$

     Construct the scalor according to Proposition 1.6.4 and the final ellipse E_f by (1.4) as

     $$E_f = S_+ S_- S_\times E_1^1 \bar{S}_\times \bar{S}_- \bar{S}_+.$$

4. Find the first intermediate ellipse E_2^1. Note that lower index shows the number of subsystem, to which ellipse belongs. Take e.g. $[0, b]$ as initial condition and find IPNS representation of the sample ellipse E_s by GAC conic fitting algorithm, [33]. In order to get the circumscribed ellipse E_2^1, we need E_s to have four intersection points with E_1^1. This can be checked easily by determining the type of the conic $(E_1^1 \wedge E_s)^* \wedge \bar{n}_+$ and we shall scale E_s by a factor $\alpha < 1$ as in (1.4) until the conic type of $(E_1^1 \wedge E_s)^* \wedge \bar{n}_+$ is two intersecting lines. Then continue.

   - Find the intersections $E_1^1 \wedge E_2^1$ according to Chapter 1.6.4.
   - Construct pair of lines p_1 and p_2 according to Remark 1.6.1 and calculate their axis $p = \frac{1}{2}(p_1 + p_2)$. To recognize the correct line one can use the inner product with the lines determined by the ellipse E_1^1 semiaxis denoted also as a and b. Indeed, $a \cdot p \leq b \cdot p$ which is clear from Figure 1.7 and from the properties of inner product similar to the scalar product of vectors. Clearly, in IPNS representation both a and p are 1-vectors.
   - Construct the intersection of p and E_1^1 by $P_{t12} = E_1 \wedge p$. Then P_{t12} is a point pair of contact points P_{t1} and P_{t2}.
   - Calculate the scaling parameter α between the ellipses E_s and E_2^1 as $\alpha = \frac{\|S P_{t1}\|}{a'}$, where a' is the length of E_s semiaxis. Note that the ellipse parameters may be easily computed from the matrix (1.9). Correctness of this calculation follows from Proposition 1.6.4.
   - Construct E_2^1 by rescaling E_s.

5. Check the intersection between E_f and E_2^i, where $i = 1, 2..$ is the number of additional ellipse in the following steps.

   (a) If $E_f \cap E_2^i \neq \varnothing \implies$ find the intersection points of all ellipses, get the path from A to B by choosing the nearest point with respect to the path evolution. This will switch to final ellipse.

   (b) If $E_f \cap E_2^i = \varnothing \implies$ calculate the scaling parameter $S P$ according to Proposition 1.6.4.

   By scaling E_1^i, E_2^i using $S P$ get new pair of circumscribed ellipses

$$E_2^{i+1} := \text{scale}(E_2^i, S P), \quad E_1^{i+1} := \text{scale}(E_1^i, S P),$$

Get intersection $E_1^{i+1} \cap E_2^{i+1}$, add points of intersection to the list of switching points and return to the beginning of the step 5 until $E_f \cap E_2^j \neq \varnothing$ for some j. This cycle constructs the sequence of ellipses from the starting ellipse to the final one.

As a result, the above algorithm provides a sequence of switching points as well as a sequence of trajectories in GAC [31]. For example of the resulting path see Figure 3.4.

3.3 Examples and comparison to the numerical methods

Let us now consider the following set of examples, which generalize the system from [39, p. 6]. The following systems describe the oscillatory problem without damping.

Example 7. Consider the switched system (3.2) in its matrix form, ie., $\dot{\boldsymbol{x}} = A_i \boldsymbol{x}$, for $i = 1, 2$, where

$$A_1 = \begin{pmatrix} 0 & 1 \\ -2 & 0 \end{pmatrix}, \quad A_2 = \begin{pmatrix} 0 & 1 \\ -\frac{1}{2} & 0 \end{pmatrix}.$$

Consider the starting point $S = [2, 5]$ and the ending point $E = [12, 22]$. We need to find the path from S to E composed of the respective system trajectories. For example of the pair of ellipses families see Figure 3.1, left, where the ellipses have a common centre and perpendicular semiaxes. In Figure 3.1, right, the resulting path can be found. Consequently, the set of switching points is calculated with the following result:

```
[0,-5.74456],[8.12404,0],[0,11.48913],[-16.24808,0],
[0,-22.97825],[23.2054167141,12.86501593890354].
```

This is a result of Python code written in a module Clifford according to the algorithm in Chapter 3.2. Note that the red points in Figure 3.1, left, form the set of points generated by Runge-Kutta method and you can see the fitted conic, too.

In order to compare the result received by the use of GAC with numerical solution, we solve the same system numerically. Instead of GAC conic fitting and searching for intersections, we use Runge-Kutta method for the next ellipse construction and for the last ellipse we get the system of two quadratic equations. For fitting the ellipse we use the least squares fitting of ellipses by Halir and Flusser [40].

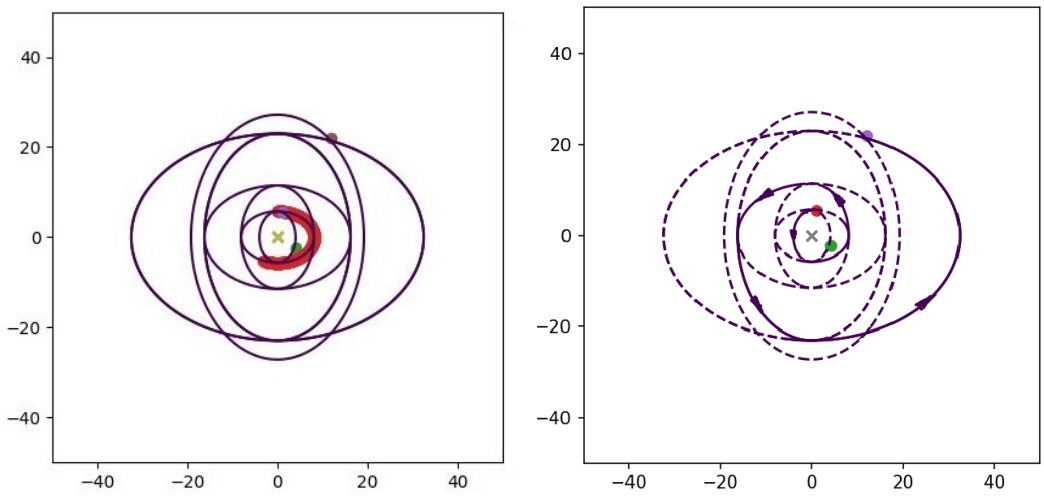

Figure 3.1: Example 7

1. Get S, E, the starting and final point

2. Find the IPNS representation of the initial ellipse E_1^1 by conic fitting algorithm. Let us denote its semiaxis by a and b.

3. Find the final ellipse E_f in by Runge-Kutta and conic fitting algorithm

4. Find the intermediate ellipse E_2^i. Note that lower index shows the number of subsystem, to which ellipse belongs. Take e.g. $[0, b]$ as initial condition and using Runge-Kutta for solving the system of differential equations with the starting point and $[0, b]$.

5. Using ellipse fitting algorithm get the needed intermediate ellipse.

6. Check the intersection between E_f and E_2^i, where $i = 1, 2..$ is the number of additional ellipse in the following steps. This is done by solving the system of quadratic equations.

   (a) If $E_f \cap E_2^i \neq \varnothing \implies$ find the intersection points of all ellipses, get the path from S to E by choosing the nearest point with respect to the path evolution. This will switch to final ellipse.

   (b) If $E_f \cap E_2^i = \varnothing \implies$ then keep constructing inscribed ellipses E_1^i and E_2^i.

Get intersection $E_1^{i+1} \cap E_2^{i+1}$, add points of intersection to the list of switching points and return to the beginning of the step 5 until $E_f \cap E_2^j \neq \varnothing$ for some j. This cycle constructs the sequence of ellipses from the starting ellipse to the final one.

As a result of the above numerical algorithm we receive the following set of switching points:

```
[0.0, 5.74456265], [8.1240384,0.0], [0.0, 11.48912529],
[16.24807681,0.0],[0.0,22.97825059],
[-21.1344899771933,12.7540843143374].
```

Let us compare the resulting coordinates with the case of using geometric algebra:

```
[0.0, 5.744562646461688], [8.12404, 0.0], [0.0, 11.48913],
[16.24808, 0.0], [0.0, 22.97825],
[-23.205416714111358,  12.86501593890354].
```

Note that the final switching point is different in the numeric case. This happens due to the fact that the calculations in the numerical solution contains a numerical error in the final numerical calculation of the ellipses intersection, which is completely avoided in the case of GAC where the intersections are obtained geometrically, for more details see Section 1.6.4.

Example 8. Let us note that numerical error increases with the increasing number of the intermediate ellipses. Every new ellipse is carrying the error from the previous step and this can lead to the differences in the set of switch points, see Figure 3.2 displaying the set of intermediate ellipses geometrically for both GAC (left) and numerical(right) solution although the difference is not quite clear. To see the error in coordinates, we add the list of respective switching points. The following list represents the respective switching points and their coordinates for numerical and GAC solution. Note that the difference between the final switching point FNUM and FGAC of the numerical method and GAC, respectively, is significant.

```
NUMERIC
[0.0, 5.744562646461688], [8.12404, 0.0], [0.0, 11.48913],
[16.24808, 0.0], [0.0, 22.97825], [32.49615, 0.0],
[0.0, 45.9565], [64.99231,  0.0], [0.0, 91.913],
FNUM=[-101.93109159592173, 29.564380018122797]
```

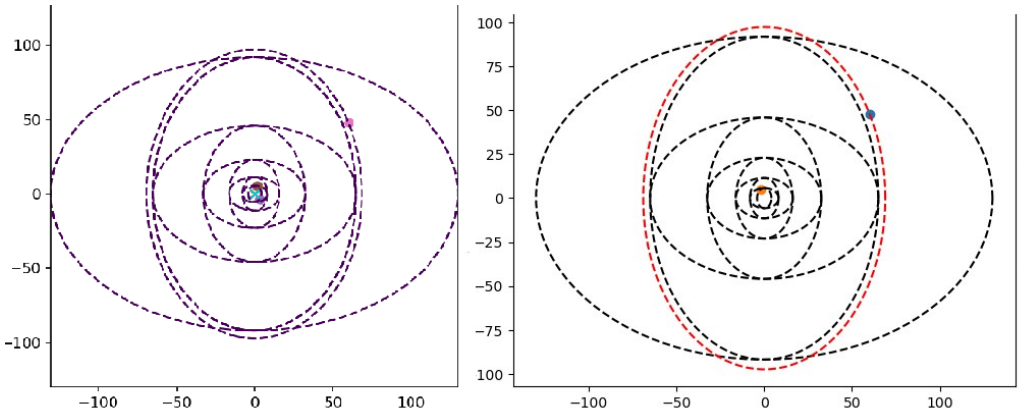

Figure 3.2: Example 8, GAC solution(left) and numeric solution(right)

```
GAC
[0.0, 5.74543306], [8.12526935, 0.0, [0.0, 11.49086611],
[16.2505387, 0.0], [0.0, 22.98173222], [32.5010774, 0.0],
[0.0, 45.96346444],[65.00215479,  0.0], [0.0, 91.92692889],
FGAC=[-89.9967425686796,26.5008143923407]
```

Let us note that even numerically we can find the switches of the system, but they may not be optimal due to the amount of switches, see the following example.

Example 9. In some cases even the number of switches can be different. If, for example, the ending point belongs to one of the ellipses of the starting family, and the number of steps is relatively large, the numeric solution can offer extra ellipse, therefore, the set of switching points is growing and the solution is not optimal with respect to the number of switches.

Figure 3.3, right, demonstrates the extra horizontal ellipse leading to new vertical ellipse as a solution, offered by numerical solution. Nevertheless, the number of switches can differ only by 1 because the length of the semiaxes of the circumscribed ellipses grows much faster than the numerical error. As a result we conclude that the numeric solution may not be optimal with respect to the number of switches.

Example 10. Now let us consider the pendulum problem with damping. The corresponding switched system is switched system $\dot{\boldsymbol{x}} = A_i \boldsymbol{x}$, $i = 1, 2$, where matrices

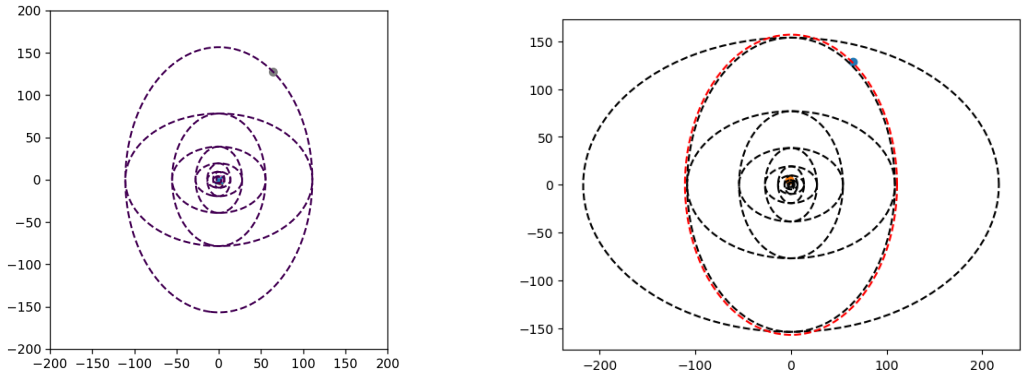

(a) GAC solution (b) Numeric solution

Figure 3.3: Example 9

of the sybsystems are given as

$$A_1 = \begin{pmatrix} 0 & 1 \\ -2 & 0 \end{pmatrix}, \quad A_2 = \begin{pmatrix} 1 & 1 \\ -2 & 1 \end{pmatrix}.$$

The starting point is $[2;5]$, and we need to find a path to the point $[30;22]$. Both of the matrices have pure imaginary eigenvalues, so the system is switching between ellipses. Ellipses of the second family are rotated. That means that the second subsystem describes one of the cases of the oscillatory system with damping. These can also produce other types of conics, e.g. spirals, but that case is not the point of our interest. The set of switching points is

```
[-2.88653912573,-3.697011208397],
[-4.23042514649,8.76807759024],
[5.98270815467, -7.662511450902],
[-8.76807759024,18.1729216252],
[-15.88149952097,-12.39990012429],
[-11.14111993673,43.01897176660]
```

and the switching path calculated in Python module Clifford can be seen in Figure 3.4.

Remark. Problems with a closed curve, ie., when the starting point coincides with the ending point, may be of particular interest. In this case, the controllability condition also applies. Let S be the starting point and let A be an arbitrary point

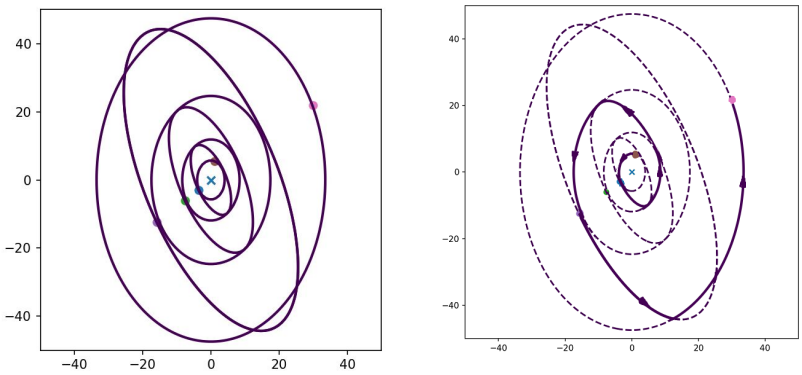

Figure 3.4: Example 10

on the phase portrait. Then the existence of a path from S to A follows from the controllability of the system. Similarly, there exists a path from A to S. Thus, we obtain a curve with a start and an end at S and passing through an arbitrary point A, see Figure 3.5.

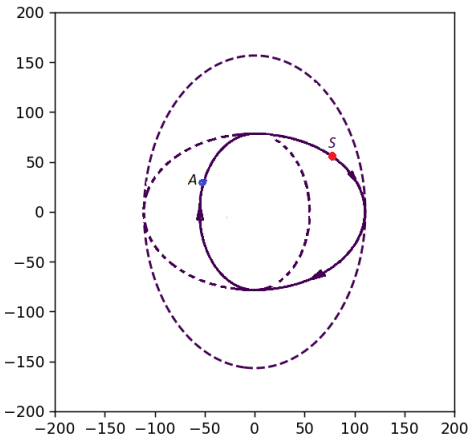

Figure 3.5: Closed curve controllability

Note that the presented algorithm is applicable for the switched systems, with subsystems, whose phase curves are intrinsic to GAC elements.

3.4 Saddle-Saddle

In the following section, the case of 2×2 matrices with both subsystems having real eigenvalues is considered. Further we will refer to this type of the switched system as Saddle-Saddle. The equilibrium point is called a Saddle under the following condition: the eigenvalues λ_1, λ_2 are real numbers of the opposite sign, ie., $\lambda_1\lambda_2 < 0$. Since one of the eigenvalues is positive, the saddle is an unstable equilibrium point. Let us suppose $\lambda_1 < 0, \lambda_2 > 0$.

The straight lines directed along the corresponding eigenvectors are called separatrices. These are the asymptotes of other phase trajectories that have the form of a hyperbola. Each of the separatrices can be associated with a certain direction of motion.

Let us consider switched system

$$\dot{\boldsymbol{x}}(t) = A_i\boldsymbol{x}(t), \quad i = 1, 2,$$

where

$$A_1 = \begin{pmatrix} 0 & 1 \\ \alpha & 0 \end{pmatrix}, \quad A_2 = \begin{pmatrix} 0 & 1 \\ 1/\alpha & 0 \end{pmatrix}, \quad \alpha > 0,\ \alpha \in \mathbb{R}.$$

Considering subsystems of the switched system separately, we get the solution of the first subsystem

$$\dot{\boldsymbol{x}}(t) = A_1(\boldsymbol{x}(t))$$

in the form

$$x_1(t) = \gamma_1 e^{\sqrt{\alpha}t} + \gamma_2 e^{\sqrt{\alpha}t}$$
$$x_2(t) = -\sqrt{\alpha}\gamma_1 e^{\sqrt{\alpha}t} + \sqrt{\alpha}\gamma_2 e^{\sqrt{\alpha}t}$$

and the solution of the second subsystem

$$\dot{\boldsymbol{x}}(t) = A_2(\boldsymbol{x}(t))$$

in the form

$$x_1(t) = \delta_1 e^{\frac{1}{\sqrt{\alpha}}t} + \delta_2 e^{\frac{1}{\sqrt{\alpha}}t}$$
$$x_2(t) = \frac{1}{\sqrt{\alpha}}\delta_1 e^{\frac{1}{\sqrt{\alpha}}t} - \frac{1}{\sqrt{\alpha}}\delta_2 e^{\frac{1}{\sqrt{\alpha}}t},$$

respectively.

For now let us fix $\alpha > 1$. Let us now consider phase portraits for both systems. We start from plotting them separately for each subsystem, and then the Figure 3.7 shows both systems together.

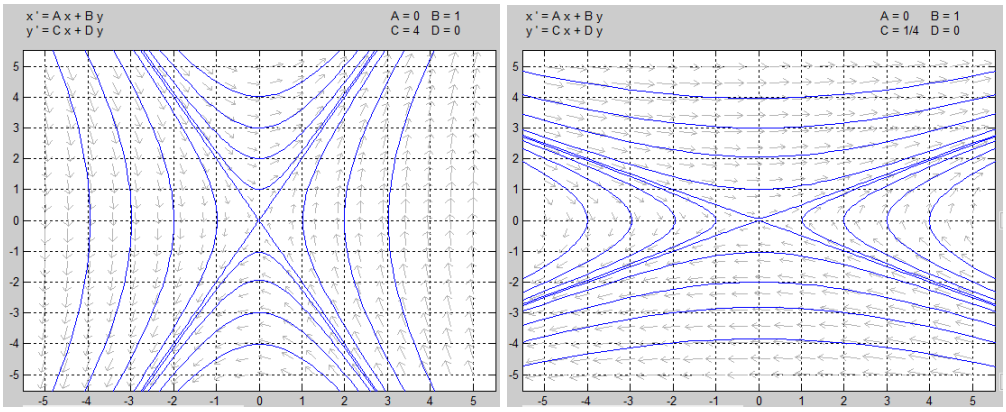

Figure 3.6: Phase portraits for first(left) and second(right) systems for $\alpha = 4$

Let us consider the phase portrait for a switched system (see Figure 3.7) and let us argue those types of the system that are not controllable. We will demonstrate it on the system's phase portrait.

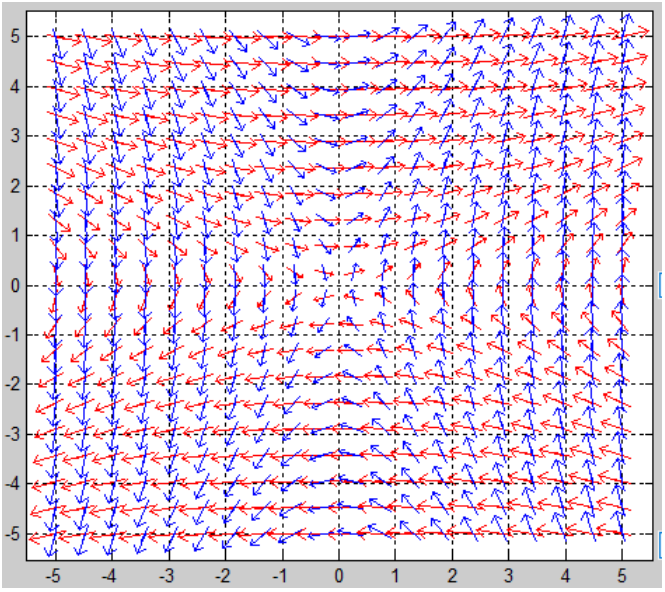

Figure 3.7: Phase portrait for switched system for $\alpha = 4$

In this case, there is no set of switching points that allows to get from points in the first and third quadrants to points in the second and fourth quadrants. Therefore, there exists at least one pair of points that cannot be connected by a trajectory.

Thus, a Saddle-Saddle type switched system is not controllable. Let us note that in the case when the algorithm for switching path construction, see 3.2, is

applied, it will be interrupted by reaching a predescribed maximal number of iterations.

3.5 Center-Saddle

In the next step, we consider a switched system, where one of the matrices has real eigenvalues of different signs (a singular point of the Saddle type), and the other has purely imaginary eigenvalues.

Let us consider switched system (3.2), where matrices take the form

$$A_1 = \begin{pmatrix} 0 & 1 \\ -\alpha & 0 \end{pmatrix}, \quad A_2 = \begin{pmatrix} 0 & 1 \\ 1/\alpha & 0 \end{pmatrix}, \quad \alpha > 0,\ \alpha \in \mathbb{R}. \tag{3.3}$$

When switched system consists of subsystems of the Center and Saddle type, the algorithm 3.2 is also applicable, but it is greatly simplified. The fact is that in this case, only two switches are enough to find the path. Let us formulate the following theorem.

Theorem 3.5.1. The switched system (2.14) with subsystems having matrices of the type (3.3) is controllable. Moreover, if the movement from the starting point corresponds to the system of the Saddle type, then it is possible to get to an arbitrary end point using two switches.

The proof follows directly from the fact that for any two axes aligned hyperbolas of the form

$$x^2 - \alpha y^2 = c^2$$

there exists an ellipse of the form

$$x^2 + \frac{y^2}{\alpha} = d^2,$$

intersecting both of the hyperbolas.

Therefore, the first step is to find the hyperbolas passing through the starting and ending points. Then the intermediate ellipse is used for the motion between them, therefore we find the needed path with 2 switches (see Figure 3.8).

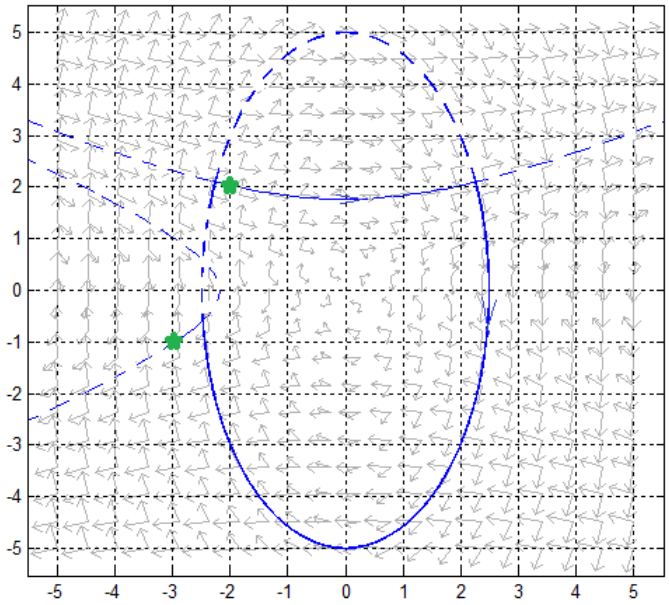

Figure 3.8: Phase portrait for system with Saddle and Center subsystems, $\alpha = 4$, Starting point [-2,2], ending point [-3,-1]

Remark. The starting point lies on the hyperbola H_1, the end point on the hyperbola H_2, respectively. We need an ellipse from the auxiliary family that will have a contact point with one of the hyperbolas and intersect with the other. To find such an ellipse, we take an instance of the auxiliary class (ellipse) and scale it until the contact point with hyperbola which semiaxis it bigger. That will guarantee us intersection with the other hyperbola. The scaling procedure is done with the scalor 1.16 by means of GAC.

3.6 Node-Node

We again consider switched system (3.2), where the system matrices take the following form

$$A_1 = \begin{pmatrix} 1 & \alpha \\ -\alpha & 1 \end{pmatrix}, \quad A_2 = \begin{pmatrix} -1 & \frac{1}{\alpha} \\ -\frac{1}{\alpha} & -1 \end{pmatrix}$$

where $\alpha > 0$, $\alpha \in \mathbb{R}$.

The eigenvalues λ_1, λ_2 of the respective subsystems are real numbers of the same sign, therefore we classify the equilibrium point as point of type Node.

The following particular cases may arise here.

3.6.1 Stable Node

In the case of Stable Node (also known as Sink) the roots λ_1, λ_2 are distinct $\lambda_1 \neq \lambda_2$ and negative.

Let us consider the phase portrait for this system. Suppose that $|\lambda_1| < |\lambda_2|$. The general solution has the form

$$\boldsymbol{x}(t) = C_1 e^{\lambda_1 t} v_1 + C_2 e^{\lambda_2 t} v_2,$$

where $v_1 = (v_{11}, v_{12})^T, v_2 = (v_{21}, v_{22})^T$ are the eigenvectors corresponding to λ_1, λ_2, respectively. As $t \to \infty$, the phase trajectories tend to the origin. Therefore the origin is equilibrium point of the type Stable Node. Let us consider it more precisely. Since

$$x_1(t) = C_1 v_{11} e^{\lambda_1 t} + C_2 v_{21} e^{\lambda_2 t},$$
$$x_2(t) = C_1 v_{12} e^{\lambda_1 t} + C_2 v_{22} e^{\lambda_2 t},$$

$$\frac{dx_2}{dx_1} = \frac{C_1 v_{12} \lambda_1 e^{\lambda_1 t} + C_2 v_{22} \lambda_2 e^{\lambda_2 t}}{C_1 v_{11} \lambda_1 e^{\lambda_1 t} + C_2 v_{21} \lambda_2 e^{\lambda_2 t}} = \frac{C_1 v_{12} \lambda_1 + C_2 v_{22} \lambda_2 e^{(\lambda_2 - \lambda_1) t}}{C_1 v_{11} \lambda_1 + C_2 v_{21} \lambda_2 e^{(\lambda_2 - \lambda_1) t}}.$$

In this case, $\lambda_2 - \lambda_1 < 0$. Therefore, the terms with the exponential function tend to zero as $t \to \infty$. As a result, for $C_1 \neq 0$, we obtain

$$\lim_{t \to \infty} \frac{dx_2}{dx_1} = \frac{v_{12}}{v_{11}},$$

ie., the phase curves get the direction of the eigenvector v_1 as $t \to \infty$. If $C_1 = 0$, the derivative at any t equals $\frac{dx_2}{dx_1} = \frac{v_{22}}{v_{12}}$, ie., the phase trajectory lies on a line directed along the eigenvector v_2 as $t \to -\infty$. The coordinates $x_1(t), x_2(t)$ tend to infinity, and the derivative $\frac{dy}{dx}$ for $C_2 \neq 0$ is of the following form:

$$\frac{dx_2}{dx_1} = \frac{C_1 v_{12} \lambda_1 e^{(\lambda_1 - \lambda_2) t} + C_2 v_{22} \lambda_2}{C_1 v_{11} \lambda_1 e^{(\lambda_1 - \lambda_2) t} + C_2 v_{21} \lambda_2} = \frac{v_{22}}{v_{21}},$$

therefore, the phase curves at the points at infinity flow in the direction to the vector v_2.

Now let us consider the switched system 2.5 with both subsystems having equilibrium point of the type Stable Node, ie.,

$$A_1 = \begin{pmatrix} -1 & 0 \\ 0 & -\alpha \end{pmatrix}, \quad A_2 = \begin{pmatrix} -1 & 0 \\ 0 & -\frac{1}{\alpha} \end{pmatrix}$$

where $\alpha > 0,\ \alpha \in \mathbb{R}$. We show the phase portraits together with some phase curves for the systems with the matrices A_1, A_2 as above separately in Figure 3.9 and the phase portraits for the same switched system in one picture, Figure 3.10.

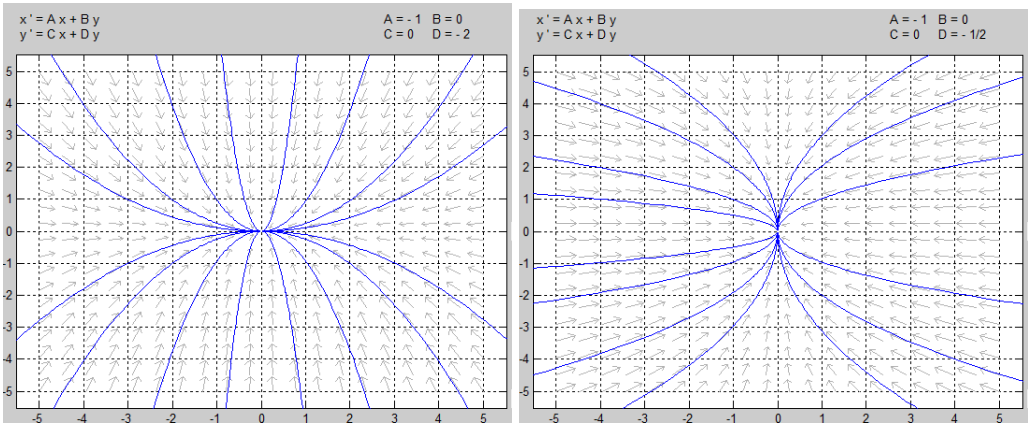

Figure 3.9: Phase portrait for both systems with $\alpha = 2$

Now let us consider both subsystems together and investigate them from the geometric point of view, see Figure 3.10.

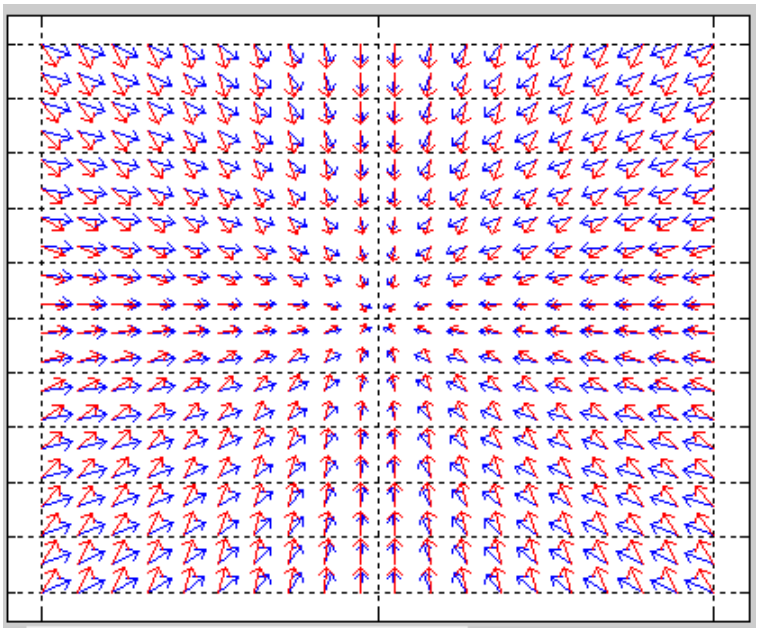

Figure 3.10: Phase portrait for switched system for $\alpha = 2$

In this case, it is impossible to leave a neighborhood of zero, so there exists no switching path if the starting point is laying closer to the origin than the ending point. Therefore, switched systems of this type are not controllable.

3.6.2 Unstable Node

The case of Unstable Node (also known as Source) is analogical to the case of Stable Node but with both corresponding eigenvalues being positive. More precisely, we consider the system (3.2) with the matrices

$$A_1 = \begin{pmatrix} 1 & 0 \\ 0 & \alpha \end{pmatrix}, \quad A_2 = \begin{pmatrix} 1 & 0 \\ 0 & \frac{1}{\alpha} \end{pmatrix}.$$

where $\alpha > 0$, $\alpha \in \mathbb{R}$.

Taking into account the geometry of the system (see Figure 3.11), note that there is no set of switching signals that allows the path from a point in $\mathbb{R}^2$ to a point that is closer to the origin. Therefore, similarly to the previous case, the system is not controllable.

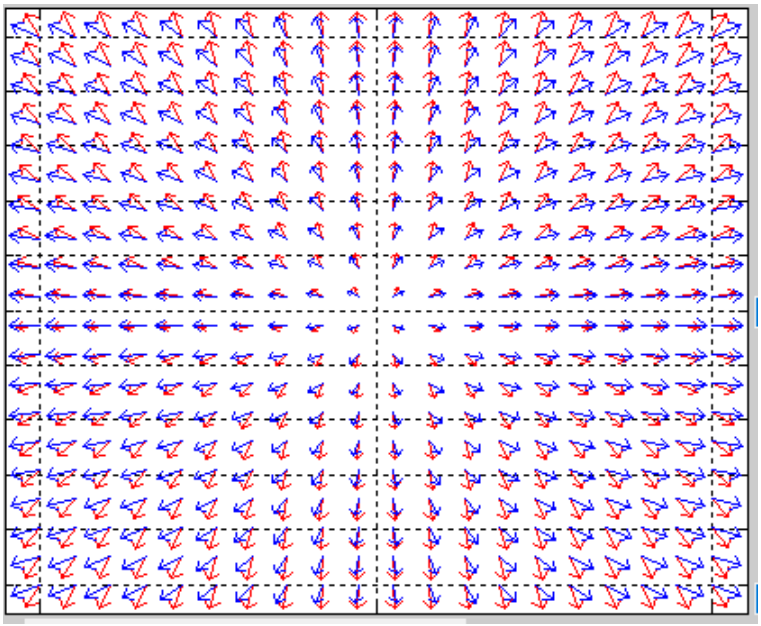

Figure 3.11: Phase portrait for switched system with $\alpha = 2$

3.6.3 Stable-Unstable Nodes

Now let us consider the combination of Stable and Unstable Nodes, ie., the system (3.2) with matrices

$$A_1 = \begin{pmatrix} -1 & 0 \\ 0 & -\alpha \end{pmatrix}, \quad A_2 = \begin{pmatrix} 1 & 0 \\ 0 & \frac{1}{\alpha} \end{pmatrix}.$$

where $\alpha > 0,\ \alpha \in \mathbb{R}$.

Let us again consider the phase portrait of the system, see Figure 3.12. From the geometric point of view, the system is controllable with the starting and ending point lying in the same quadrant. But in general, the switching path does not exist for any two points. For example, the movement from the point $[1, 2]$ to the point $[-1, 2]$ can be taken into account only if we formally consider the origin to be a switching point. But this point is not feasible for finite t, therefore, this type of the switched systems is also not controllable.

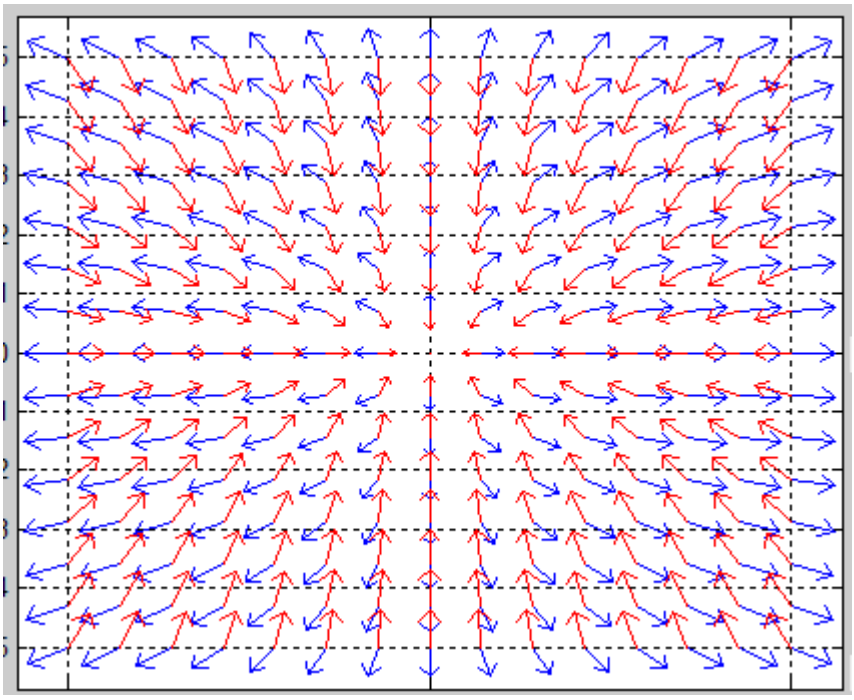

Figure 3.12: Phase portrait for switched system with $\alpha = 2$

3.6.4 Dicritical Node

Now let us consider a specific case, precisely the case of Dicritical Node. It is again the switched system (3.2), where the eigenvalues of both system matrices are equal and nonzero, ie.:

$$\lambda_1 = \lambda_2 = \lambda \neq 0.$$

The system has a basis of two eigenvectors, ie., the geometric multiplicity of the eigenvalue λ is 2, in other words the dimension of the eigenspace of A is equal to 2. This situation occurs for systems of the form

$$\frac{dx_1}{dt} = \lambda x_1, \quad \frac{dx_2}{dt} = \lambda x_2$$

as the first subsystem with eigenvalue λ and

$$\frac{dx_1}{dt} = \nu x_1, \quad \frac{dx_2}{dt} = \nu x_2$$

as the second subsystem with eigenvalue ν, respectively. Consider first subsystem in details. The direction of the phase trajectories depends on the sign of λ. Here

the following two cases can arise: for $\lambda_1 = \lambda_2 = \lambda < 0$, the equilibrium is called a Stable Dicritical Node and for $\lambda_1 = \lambda_2 = \lambda > 0$, Unstable Dicritical Node. Phase portraits for both cases are demonstrated separately on Figure 3.13.

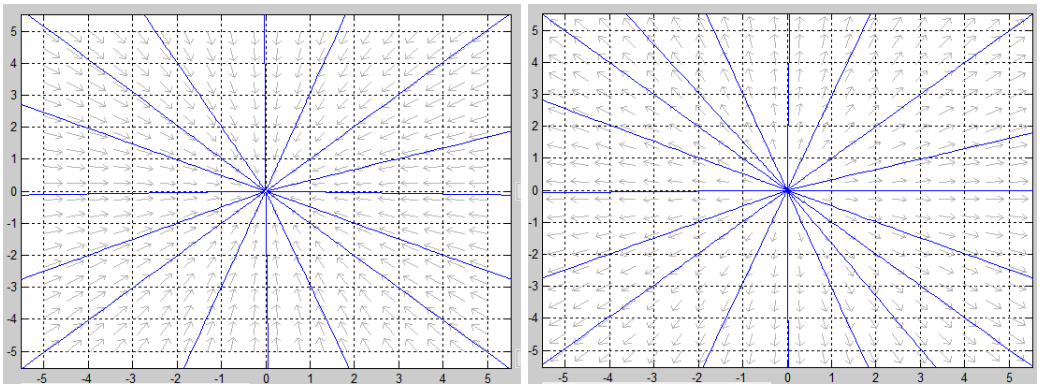

Figure 3.13: Phase portrait for both systems for $\alpha = 2$

This leads to a conclusion that this type of switched system is not controllable. A switch is between two different trajectories is possible in the equilibrium point only, but this point is not feasible. If the two trajectories are identical with opposite orientation, then the motion is allowed within this particular trajectory only. Therefore, the system is not controllable.

3.7 Center-Node

We again consider switched system (3.2) with the system matrices of the following form

$$A_1 = \begin{pmatrix} 0 & 1 \\ -\alpha & 0 \end{pmatrix}, \quad A_2 = \begin{pmatrix} 1 & \alpha \\ -\alpha & 1 \end{pmatrix}, \quad \alpha > 0,\ \alpha \in \mathbb{R}. \tag{3.4}$$

The first subsystem matrix A_1 has pure imaginary eigenvalues, ie., it is classified as the type Center. The second subsystem matrix A_2 has real eigenvalues, both positive or both negative, ie., it is classified as the type Node.

From geometrical point of view, we again conclude that the switched system will not be controllable. Similarly to the previous not controllable cases, the Center type system does not allow movement towards the origin (see Figure 3.14). Therefore there exists at least one pair of points that cannot be connected by a path, e.g., the starting point being further from the origin than the end point, and thus the system is not controllable.

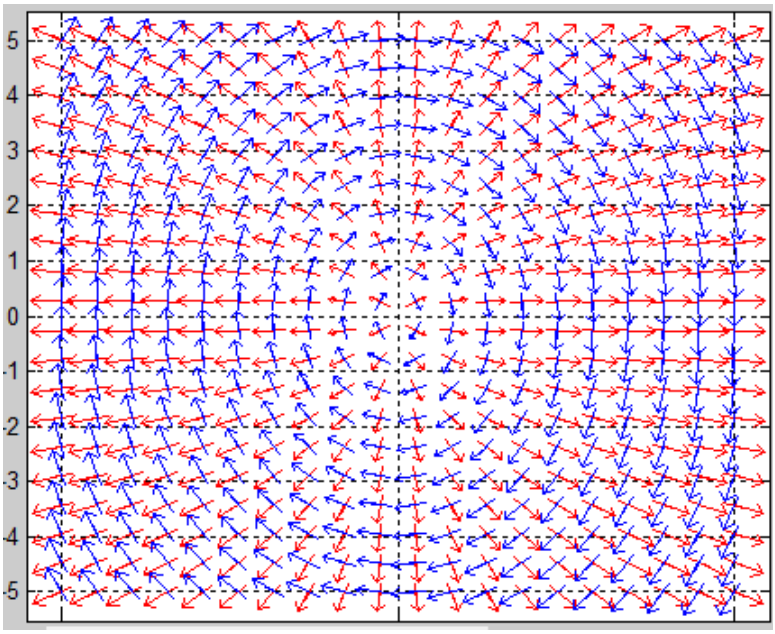

Figure 3.14: Phase portrait for system with Node and Center subsystems, $\alpha = 2$

3.8 Summary of Chapter 3

The Chapter describes the controllability of the 2×2 switched systems with regular matrices of each subsystem by the means of Geometric Algebra. It was demonstrated that the use of GAC for construction of switching points of 2D switched systems leads to the solution that is optimal with respect to the number of switches. From the geometric nature of our approach we can see that the number of switches can only differ by 1 from the numerical solution but also the numerical error for particular switches must be taken into account. We provided examples with axes aligned ellipses but from the description of GAC it is clear, that their approach will handle rotated conics of any type as well, in which case numerical solution will carry even larger error.

Chapter 4

Cases laying out of GAC

In the previous chapter we considered the cases where the phase curves of the subsystems of the switched system are intrinsic to GAC, ie., conic sections.

The aim of the following chapter is to describe particular systems whose phase portrait contains 2D curves, not being conic sections (for example, spirals), therefore, laying out of GAC.

Upon further investigation, it turned out that among the switched systems with regular 2x2 matrices, except the systems described in the previous Chapter, controllable can be also switched systems corresponding to switch between matrices with equilibrium point of the type stable and unstable Focuses (λ_1, λ_2 are complex numbers $\mathrm{Re}\lambda_1 = \mathrm{Re}\lambda_2 \neq 0$) and partially controllable systems are systems, which have switches between Saddle (λ_1, λ_2 are real numbers of the opposite sign $\lambda_1\lambda_2 < 0$) and Focus (λ_1, λ_2 are complex numbers $Re\lambda_1 = Re\lambda_2 \neq 0$). Now let us consider those cases in detail.

4.1 Focus-Focus

The equilibrium point of dynamical system of the form

$$\dot{\boldsymbol{x}} = A\boldsymbol{x},\ A \in \mathcal{M}at_2(\mathbb{R}),$$

is called a Focus under the following condition: the eigenvalues λ_1, λ_2 of the matrix A are complex numbers with non-zero real part. If the matrix A is composed of real numbers, the complex roots the characteristic polynomial are conjugate complex numbers: $\lambda_{1,2} = a \pm ib$.

The solution $\boldsymbol{x}(t)$ corresponding to the eigenvalue $\lambda_1 = a + ib$ is of the form

$$\boldsymbol{x}(t) = e^{\lambda_1 t}\boldsymbol{v}_1 = e^{(a+ib)t}(\boldsymbol{u} + i\boldsymbol{w})$$

where $\boldsymbol{v}_1 = \boldsymbol{u}+i\boldsymbol{w}$ is the complex-valued eigenvector associated with the eigenvalue λ_1, $\boldsymbol{u}$ and $\boldsymbol{w}$ are 2D real vectors. As a result, we obtain

$$\boldsymbol{x}(t) = e^{at}e^{ibt}(\boldsymbol{u} + i\boldsymbol{w}) = e^{at}(\cos bt + i\sin b)(\boldsymbol{u} + i\boldsymbol{w}) =$$
$$= e^{at}(\boldsymbol{u}\cos bt - \boldsymbol{w}\sin bt)) + ie^{at}(\boldsymbol{w}\cos(bt + \boldsymbol{u}\sin bt)).$$

The real and imaginary parts in the above expression form real solution

$$\boldsymbol{x}(t) = C_1\mathrm{Re}(\boldsymbol{x}(t)) + C_2\mathrm{Im}(\boldsymbol{x}(t)) =$$
$$= e^{at}(\boldsymbol{u}(C_1\cos bt + C_2\sin bt) + \boldsymbol{w}(C_1\cos bt - C_2\sin bt)),\ C_1, C_2 \in \mathbb{R}.$$

If we set the constants $C_1 = C\sin\delta,\quad C_2 = C\cos\delta,\ C \in \mathbb{R}$, where δ is an auxiliary angle, then the solution can be rewritten as

$$\boldsymbol{x}(t) = Ce^{at}(\boldsymbol{u}(C_1\sin\delta\cos bt + C_2\cos\delta\sin bt) + \boldsymbol{w}C_1\cos\delta\cos bt + C_2\sin\delta\sin bt) =$$
$$= Ce^{at}(\boldsymbol{u}\sin(bt+\delta) + \boldsymbol{w}\cos(bt+\delta)).$$

Thus, the solution $\boldsymbol{x}(t)$ can be expressed in the basis of vectors $\boldsymbol{u}$ and $\boldsymbol{w}$:

$$\boldsymbol{x}(t) = \mu(t)\boldsymbol{u} + \nu(t)\boldsymbol{w},$$
$$\mu(t) = Ce^{at}\sin(bt+\delta),$$
$$\nu(t) = Ce^{at}\cos(bt+\delta).$$

Therefore, the phase trajectories are spirals. In the case $\mathrm{Re}(\lambda_1) = a < 0$ and $\mathrm{Re}(\lambda_2) = a < 0$, the spirals twist in the direction towards the equilibrium point, which is then called a Stable Focus. Similarly, in the case of $a > 0$, the equilibrium point is an Unstable Focus.

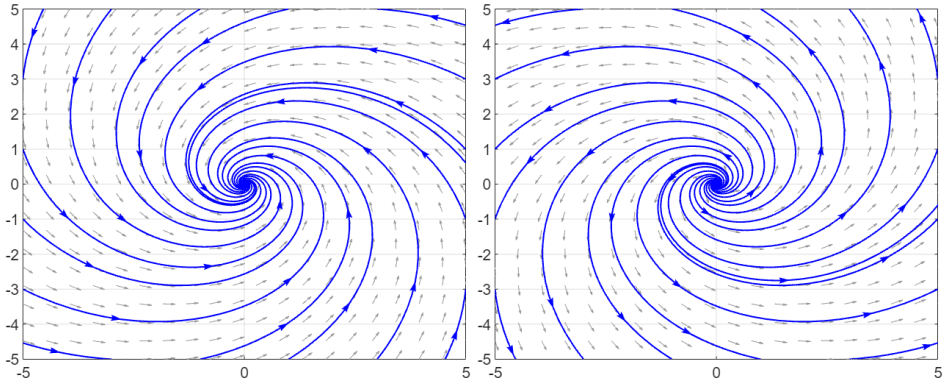

Figure 4.1: Phase portrait for Stable Focus (left), and Unstable Focus (right), $\alpha = 2$

4.1.1 Unstable Focus

Let us consider a switched system (3.2) with two subsystem matrices

$$A_1 = \begin{pmatrix} 1 & -\alpha \\ \alpha & 1 \end{pmatrix}, \quad A_2 = \begin{pmatrix} 1 & -\frac{1}{\alpha} \\ \frac{1}{\alpha} & 1 \end{pmatrix}$$

where $\alpha > 0$, $\alpha \in \mathbb{R}$. Both subsystems are classified as Unstable Focus (also known as Spiral Source).

Let us investigate the phase portrait for given above switched system (see Figure 4.2, right) and let us argue those types of the system that are not controllable. We will demonstrate it on the system's phase portrait.

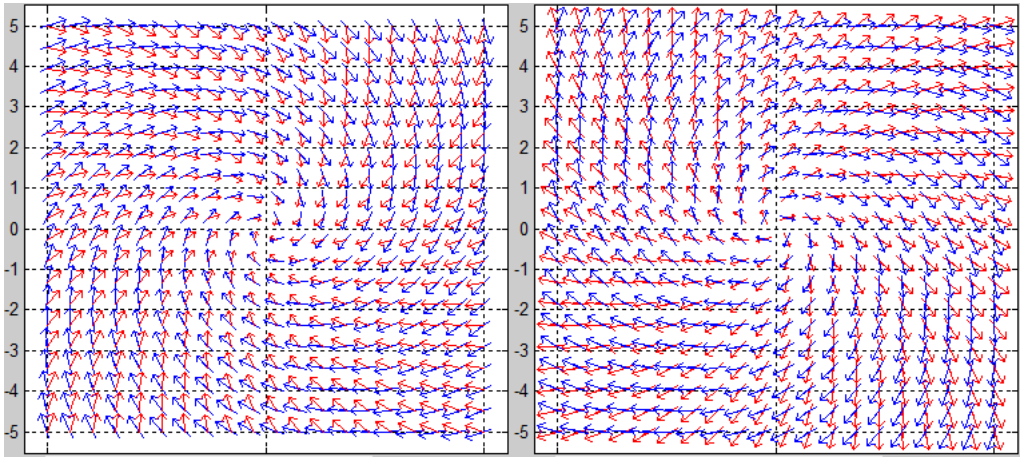

Figure 4.2: Phase portrait for switched system with Stable Focus (left), and Unstable Focus (right), $\alpha = 2$

In this case, there is no set of switching points that allows to get from a point laying far from the origin to the points in the neighborhood of zero. Therefore, there exists at least one pair of points that cannot be connected by a trajectory.

Thus, the system is not controllable.

4.1.2 Stable Focus

Let us consider a switched system (3.2) with two subsystem matrices

$$A_1 = \begin{pmatrix} -1 & \alpha \\ -\alpha & -1 \end{pmatrix}, \quad A_2 = \begin{pmatrix} -1 & \frac{1}{\alpha} \\ -\frac{1}{\alpha} & -1 \end{pmatrix},$$

where $\alpha > 0$, $\alpha \in \mathbb{R}$. Each subsystem is classified as Stable Focus (also known as Spiral Sink).

Let us consider the phase portrait for a switched system (see Figure 4.2, left) and let us argue those types of the system that are also not controllable. We will demonstrate it on the system's phase portrait. In this case, there is no set of switching points that allows to leave the neighborhood of zero. Therefore, there exists at least one pair of points that cannot be connected by a trajectory.

Thus, switched systems of this type are also not controllable.

4.1.3 Stable-Unstable Focus

Now let us investigate case of switching between systems with stable and unstable focuses. Let us consider the system (3.2), with the following matrices

$$A_1 = \begin{pmatrix} 1 & \alpha \\ -\alpha & 1 \end{pmatrix}, \quad A_2 = \begin{pmatrix} -1 & \frac{1}{\alpha} \\ -\frac{1}{\alpha} & -1 \end{pmatrix},$$

where $\alpha > 0$, $\alpha \in \mathbb{R}$. As an example, see Figure 4.3 for a phase portrait of a switched system in question and let us demonstrate on an example that for such system it is always possible to find a control for any pair of starting and end points.

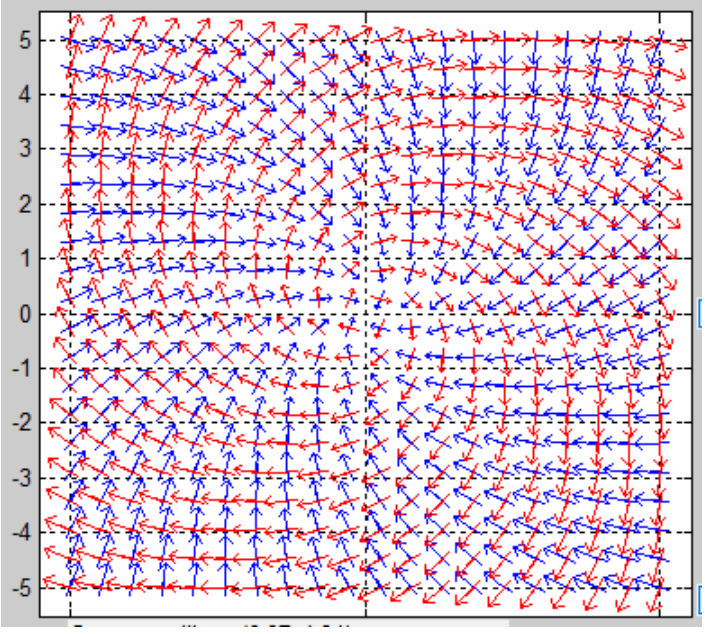

Figure 4.3: Phase portraits for systems with Stable and Unstable Focus, $\alpha = 2$

Example 11. Let us consider the system (3.2) with the following particular matrices, ie., we choose $\alpha = 2$:

$$A_1 = \begin{pmatrix} 1 & 2 \\ -2 & 1 \end{pmatrix}, \quad A_2 = \begin{pmatrix} -1 & \frac{1}{2} \\ -\frac{1}{2} & -1 \end{pmatrix}.$$

Let the starting point be $S = [-2; -1.1]$ and the ending point $E = [1; 2.4]$. We start from finding the corresponding spirals passing through S and E, respectively. The switching path is then constructed by switching between the spirals in arbitrary points with the final switch given by the intersection with the spiral containing the endpoint. For instance, the set of switching points can be the following:

```
[-2.7352;3.9998], [-0.5613;2.0000], [3.1032;2.0451],
[2.2142;0.8132], [2.6106;-1.2371].
```

The corresponding switching path is demonstrated in Figure 4.4.

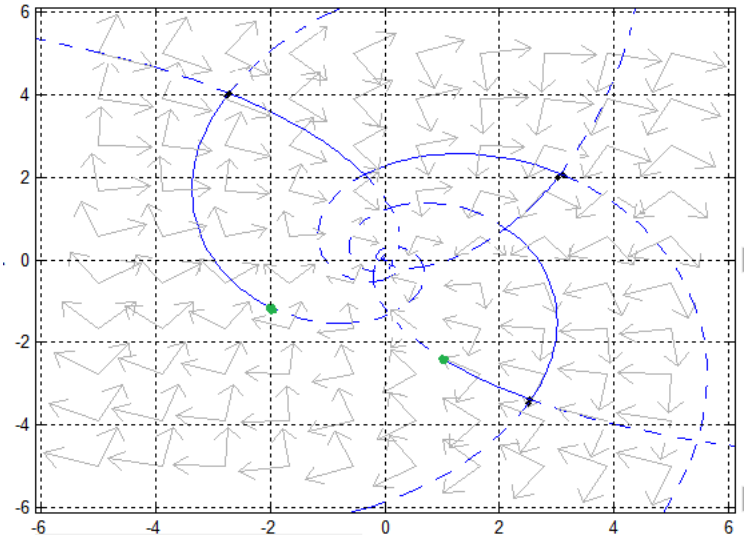

Figure 4.4: Example 11, $\alpha = 2$

Note that due to the different directions of the spirals any two points can be connected by a path containing finite number of switches. Moreover, with respect to the minimal number of switches, any two points may be connected by a switching path containing just one switch. The reason is that two spirals corresponding to different subsystems have infinitely many intersections and therefore it is always possible to choose a switch which will consequently take us to the endpoint.

Note that this choice may lead to undesirably long time. In conclusion, our system is controllable and from the geometrical point of view, the switched system of the type Stable and Unstable Focus is controllable.

4.2 Saddle-Focus

Let us consider a switched system (3.2) with the subsystem matrices of the form

$$A_1 = \begin{pmatrix} 0 & 1 \\ \alpha & 0 \end{pmatrix}, \quad A_2 = \begin{pmatrix} -1 & \frac{1}{\alpha} \\ -\frac{1}{\alpha} & -1 \end{pmatrix},$$

where $\alpha > 0$, $\alpha \in \mathbb{R}$. This case corresponds to the switch between Saddle and Stable Focus type subsystems, respectively.

For this system, two cases may arise, ie., $0 < \alpha < 1$ and $\alpha > 1$.

First, for $0 < \alpha < 1$, due to the orientation of the spiral, the system is controllable everywhere except the equilibrium point which is unreachable. This is similar to the case Center-Saddle, for more details see 3.5.

Second, for $\alpha > 1$, there is no set of switching points that allows to get from the first (third) quadrant to the second (fourth) quadrants, respectively. Therefore, there exists at least one pair of points that cannot be connected by a trajectory. Thus, a Saddle-Saddle type switched system is not controllable for $\alpha > 1$.

Therefore, the controllability of the system depends on the value of real part of the Saddle system's eigenvalue $\mathrm{Re}\lambda = \alpha$. Those systems we classify as controllable under condition.

If in the previous system, Stable Focus is changed for Unstable Focus, ie., the subsystem matrices are of the form

$$A_1 = \begin{pmatrix} 0 & 1 \\ \alpha & 0 \end{pmatrix}, \quad A_2 = \begin{pmatrix} 1 & \frac{1}{\alpha} \\ -\frac{1}{\alpha} & 1 \end{pmatrix},$$

controllability is guaranteed for $\alpha > 1$ except the equilibrium point, while for $0 < \alpha < 1$, the system is not controllable. Again, those systems are classified as controllable under condition.

Figure 4.5 demonstrates the phase portraits for parameter $\alpha = 2$ for Saddle type system combined with Unstable Focus (left) and with Stable Focus (right). It can be easily observed from the form of the phase portraits that the first system is controllable except the unreachable equilibrium point while the second system is not controllable.

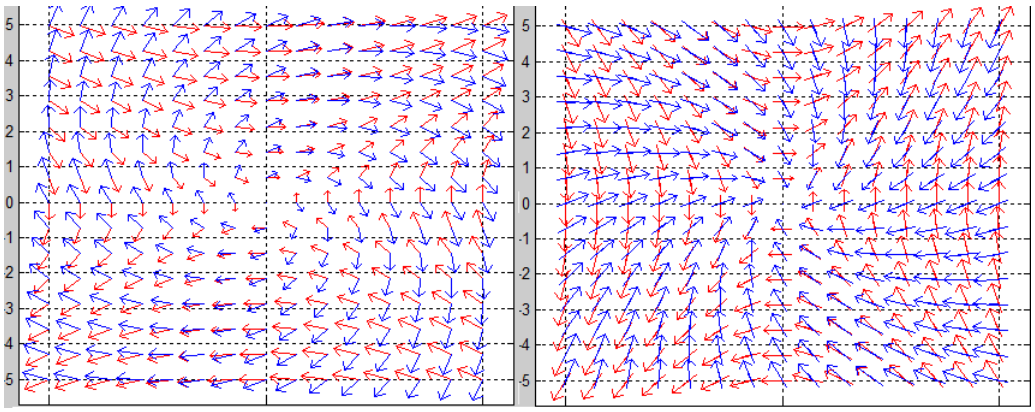

Figure 4.5: Saddle and Unstable Focus subsystems and Saddle and Stable Focus, $\alpha = 2$

4.3 Node-Focus

Let us consider a switched system (3.2), with the subsystem matrices of the form

$$A_1 = \begin{pmatrix} 1 & \alpha \\ -\alpha & 1 \end{pmatrix}, \quad A_2 = \begin{pmatrix} -1 & \frac{1}{\alpha} \\ -\frac{1}{\alpha} & -1 \end{pmatrix},$$

where $\alpha > 0$, $\alpha \in \mathbb{R}$. This case corresponds to the switch between Stable Node and Stable Focus type subsystems. Let us consider the phase portrait for a switched system depicted in Figure 4.6. Clearly, it demonstrates that such system is not controllable because no motion from the origin is allowed, more precisely, every allowed trajectory tends to the origin. Therefore, there exists at least one pair of points that cannot be connected by a trajectory. Thus, the system is not controllable.

4.4 Summary of Chapter 4

The Chapter describes the controllability of the 2×2 switched systems with regular matrices of each subsystem, whose phase portraits are not conic sections. Concrete examples and phase portraits were utilized to illustrate the controllability characteristics of different system configurations. It was demonstrated that the only controllable systems from cases laying out of GAC are the systems, which are the combination of Stable and Unstable focuses. The switched systems with

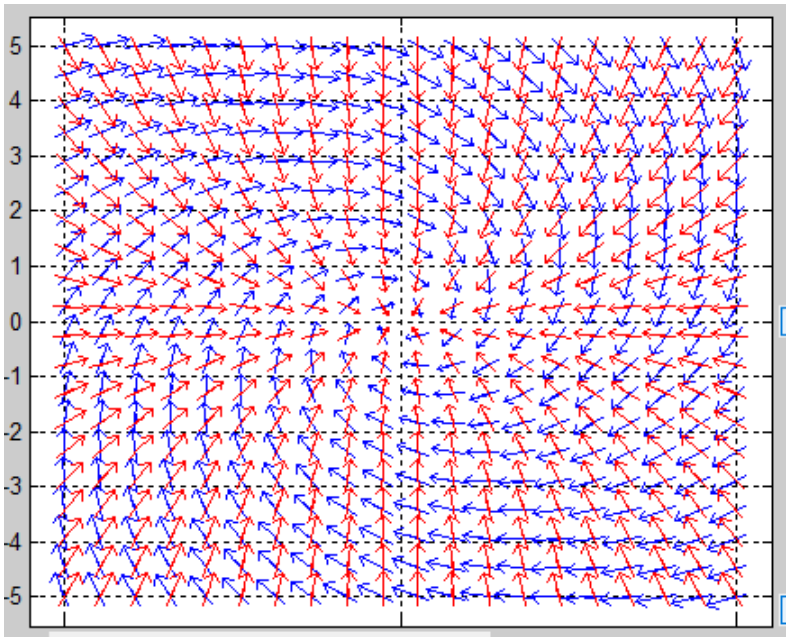

Figure 4.6: Phase portrait for system with Stable Node and Stable Focus subsystems, $\alpha = 2$

subsystem matrices's curves of the types Saddle and Focus are "controllable under condition", ie., dependent on the constant. Those systems were found to be controllable only within certain parameter ranges, contingent upon the real part of the Saddle system's eigenvalue.

Chapter 5

Results

As a result we get the following table that shows which type of switched system is controllable. For example, switched systems with matrices of the type Center-Center (both matrices have pure complex eigenvalues), are controllable, while switched systems with matrices of the type Saddle-Saddle(both matrices have real eigenvalues) are not controllable.

Table 5.1: Controllability of the switched 2x2 systems

A_1 n A_2		**Center**	**Saddle**	**Node**		**Focus**	
				Stable	**Unstable**	**Stable**	**Unstable**
Center		+	+	-	-	-	-
Saddle		+	-	-	-	controllable under condition	controllable under condition
Node	**Stable**	-	-	-	-	-	-
	Unstable	-	-	-	-	-	-
Focus	**Stable**	-	controllable under condition	-	-	-	+
	Unstable	-	controllable under condition	-	-	+	-

Therefore, the only controllable types of the switched systems are the combination of Center and Saddle, Center and Center, Stable and Unstable focuses. The switched systems with subsystem matrices's curves of the types Saddle and Focus are "controllable under condition".

Chapter 6

Conclusions

The thesis dealt with the controllability of the 2×2 switched systems with regular matrices of each of two subsystems. For the systems whose phase trajectories are conics (which are the elements of GAC), the Geometric Algebra approach was used. It was demonstrated that the use of GAC for construction of switching paths of 2D switched systems leads to the solution that is optimal with respect to the number of switches.

We demonstrated a complete geometric algorithm for a system with two families of axes–aligned, centralized ellipses in Example 5, where we showed symbolic and Python calculations, respectively. In addition, we used a property of GAC that it contains a two–dimensional conformal geometric algebra CRA, where our calculations were completed. This case corresponds to an oscillatory switched system without damping. But our approach applies also for damped systems where the integral curves are formed by rotated ellipses, ie., non axes–aligned, which we demonstrated in Examples 3 and 10. Also in this case no solver was needed because, in the system of two quadratic equations describing the ellipses' intersections, we replaced an ellipse equation by a line equation which reduced the degree and allowed analytic solution. Note that both approaches exploit the elegance of conics manipulation in GAC by constructing a pair of lines containing the intersecting points and circumscribed ellipses simply calculated by GAC scaling with a factor determined according to Proposition 1.6.4. Let us point out that even the preparation of initial trajectories is highly geometric. Fitting a conic with prescribed properties in GAC eliminates an error in numerical solution to our switched system. Indeed, all trajectories will be precisely of a given type, ie., co–centred and axes–aligned. Consequent GAC transformations do not change these properties and do not input any numerical errors. Therefore, the only place

for a rounding error is the calculation of fractions and square roots because all operations in GAC may be converted to sums of products, [28, 41].

Using the geometric nature of our approach, we demonstrated that the number of switches can only differ by 1 from the numerical solution but also the numerical error for particular switches must be taken into account. We provided examples with axes aligned ellipses but from the description of GAC it is clear, that this approach will handle rotated conics of any type as well, in which case numerical solution will carry even larger error.

Therefore, the advantages of using GAC lies in the following: The GA approach speeds up algorithms, eliminates the need for numerical solvers, reduces computational complexity, minimizes numerical errors, and allows for a coordinate-free formulation.

Classification of switched systems controllability was provided based on their geometric properties. It was proved that the only controllable systems are systems of the type Center-Center, Center-Saddle and Stable-Unstable focuses. The switched systems of type Saddle-Focus are "controlled under condition". For controllable switched systems, the controlling algorithm based on the GAC primitives and their transformations was introduced. The proposed approach creates possibility of passing from the classical solution of the controllability problem for switched systems to a geometric one, using the type of phase trajectory.

It was demonstrated that GAC as a research tool speeds up the algorithm and minimizes numerical errors. Controlling algorithms for controllable systems with elliptical, hyperbolic or combined phase trajectories based on GAC were developed. The advantage of this approach is the minimization of computational errors due to the solver-free method and minimization of number of switches.

The research was done for the systems switching between two matrices, but it can be generalized for arbitrary number of subsystems. Algorithm 3.2 is then applied on two consequent subsystems, respectively.

Overall, the thesis demonstrated the effectiveness of using Geometric Algebra for analyzing and controlling 2×2 switched dynamical systems, offering advantages in efficiency, accuracy, and simplicity of implementation.

Geometric Algebra (GA) provides a comprehensive mathematical framework for handling geometric operations efficiently. Originating from Grassmann algebras and Clifford algebras, GA unifies geometric primitives and transformations into a single algebraic structure, facilitating geometric analysis and manipulation. Key concepts include representing geometric entities using multivectors and utilizing outer, inner, and geometric product operations for manipulation.

The controllability of 2×2 switched systems with regular matrices is addressed

using Geometric Algebra. GA aids in constructing optimal switching points, minimizing the number of switches required. The approach is demonstrated with examples of axes-aligned ellipses, showcasing its effectiveness even with rotated conics.

A novel algorithm for optimal control of switched dynamical systems with purely imaginary eigenvalues is proposed. This algorithm utilizes Geometric Algebra for Conics (GAC) to construct switching paths consisting of circumscribed ellipses, minimizing numerical errors and eliminating the need for solvers.

The work highlights the geometric nature of the approach, emphasizing its ability to handle various system configurations and minimize computational errors. It also discusses the formulation of controlling algorithms mainly using GAC operations.

Bibliography

[1] L. Liu, Y.-J. Liu, D. Li, S. Tong, Z. Wang, Barrier lyapunov function-based adaptive fuzzy ftc for switched systems and its applications to resistance–inductance–capacitance circuit system, IEEE transactions on cybernetics 50 (8) (2019) 3491–3502.

[2] M. Vidyasagar, Nonlinear System Analysis, Prentice Hall, Eaglewood Cliffs, 2nd ed., New Jersey, 1993.

[3] Z. Sun, S. Sam Ge, Stability Theory of Switched Dynamical Systems, Springer-Verlag London, New York, 2011.

[4] P. Colaneri, Analysis and Control of Linear Switched Systems, Politecnico di Milano, Italy, 2018.

[5] Y. Lin, E. D. Sontag, Y. Wang, A smooth converse Lyapunov theorem for robust stability, SIAM Journal on Control and Optimization 34 (1) (1996) 124–160.

[6] Z.-P. Jiang, Y. Wang, A converse Lyapunov theorem for discrete-time systems with disturbances, Systems and Control Letters 45 (1) (2002) 49–58.

[7] M. Niezabitowski, A. Czornik, J. Klamka, Stability and controllability of switched systems, Bulletin of the Polish Academy of Sciences, Technical Sciences 61 (2013) 547–555.

[8] A. Lyapunov, General problem of motion stability, Kharkov, 1898.

[9] Q. Lin, R. Loxton, K. L. Teo, Optimal control of nonlinear switched systems: Computational methods and applications, Journal of the Operations Research Society of China 1 (3) (2013) 275–311.

[10] D. Liberzon, R. Tempo, Switched systems, common Lyapunov functions, and gradient algorithms, IEEE Trans. Automat. Control 49 (2004) 990–994.

[11] D. Liberzon, Switching in Systems and Control, Birkhauser, Boston, 2003.

[12] X. Ding, X. Liu, On stabilizability of switched positive linear systems under state-dependent switching, Applied Mathematics and Computation 307 (2017) 92–101. doi:https://doi.org/10.1016/j.amc.2017.03.007. URL https://www.sciencedirect.com/science/article/pii/S0096300317301789

[13] Y. Han, Y. Zhao, P. Wang, Finite-time rate anti-bump switching control for switched systems, Applied Mathematics and Computation 401 (2021) 126086. doi:https://doi.org/10.1016/j.amc.2021.126086. URL https://www.sciencedirect.com/science/article/pii/S009630032100134X

[14] U. A. Nasir, Dynamic Systems and Control with Applications, University of Ottawa, Canada, 2006.

[15] T. Seidman, Optimal control of a diffusion/reaction/switching system, Evolution Equations and Control Theory [electronic only] 4 (2013). doi:10.3934/eect.2013.2.723.

[16] J. Hrdina, A. Návrat, P. Vašík, Geometric algebra for conics, Adv. Appl. Clifford Algebras 28 (66) (2018). doi:https://doi.org/10.1007/s00006-018-0879-2.

[17] R. Easter, E. Hitzer, Double conformal geometric algebra, Adv. Appl. Clifford Algebras 27 (3) (2017) 2175–2199.

[18] J. Hrdina, A. Návrat, P. Vašík, Conic fitting in geometric algebra setting, Adv. Appl. Clifford Algebras 29 (72) (2019). doi:https://doi.org/10.1007/s00006-019-0989-5.

[19] R. L. Bishop, S. I. Goldberg, Tensor analysis on manifolds, Courier Corporation, 2012.

[20] A. L. Mandolesi, Blade products and angles between subspaces, Advances in Applied Clifford Algebras 31 (5) (2021) 69.

[21] C. Perwass, Geometric Algebra with Applications in Engineering, Springer Verlag, 2009.

[22] D. Hestenes, Space-time algebra, Gordon and Breach, New York, 1966.

[23] L. Gonzalez-Jimenez, O. Carbajal-Espinosa, A. Loukianov, E. Bayro-Corrochano, Robust pose control of robot manipulators using conformal geometric algebra, Adv. Appl. Clifford Algebras 24 (2) (2014) 533–552.

[24] J. Hrdina, A. Návrat, P. Vašík, R. Matoušek, Geometric algebras for uniform colour spaces, Math. Meth. Appl. Sci. (2017). doi:https://doi.org/10.1002/mma.4489.

[25] L. Dorst, D. Fontjine, S. Mann, Geometric algebra for computer science: an object-oriented approach to geometry, Rev. ed. Burlington, Mass.: Morgan Kaufmann Publishers, Morgan Kaufmann series in computer graphics., 2007.

[26] D. Hildenbrand, Introduction to Geometric Algebra Computing, Chapman and Hall/CRC, USA, 2018.

[27] P. Lounesto, Clifford Algebra and Spinors, CUP,2nd edn., Cambridge., 2006.

[28] R. Byrtus, A. Derevianko, P. Vašík, D. Hildenbrand, C. Steinmetz, On specific conic intersections in gac and symbolic calculations in gaalopweb, Advances in Applied Clifford Algebras 32 (02 2022). doi:10.1007/s00006-021-01182-z.

[29] J. H. Smith, An Introduction to the Study of Geometrical Conic Sections, Longmans Green, 1887.

[30] G. Korn, T. Korn, Mathematical Handbook for Scientists and Engineers: Definitions, Theorems, and Formulas for Reference and Review, Dover Civil and Mechanical Engineering Series, Dover Publications, 2000.
URL https://books.google.cz/books?id=xHNd5zCXt-EC

[31] A. Derevianko, P. Vašík, Solver-free optimal control for linear dynamical switched system by means of geometric algebra, Mathematical Methods in the Applied Sciences 47 (3) (2024) 1274–1288.

[32] J. Richter-Gebert, Perspectives on Projective Geometry, Springer Berlin Heidelberg, Berlin, Heidelberg, 2011.

[33] P. Loučka, P. Vašík, On multi-conditioned conic fitting in geometric algebra for conics, Advances in Applied Clifford Algebras 33 (3) (2023) 31.

[34] R. B. Easter, E. Hitzer, Double conformal geometric algebra, Advances in Applied Clifford Algebras 27 (2017) 2175–2199.

[35] M. W. Hirsch, S. Smale, R. L. Devaney, Differential equations, dynamical systems, and an introduction to chaos, Academic press, 2012.

[36] J. Stewart, D. K. Clegg, S. Watson, Calculus: early transcendentals, Cengage Learning, 2020.

[37] I. Gosea, M. Petreczky, A. Antoulas, C. Fiter, Balanced truncation for linear switched systems, Advances in Computational Mathematics 44 (12 2018). doi:10.1007/s10444-018-9610-z.

[38] A. Derevianko, V. Korobov, Controllability of the given switched linear system of special type, Visnyk of V.N.Karazin Kharkiv National University Ser. Mathematics, Applied Mathematics and Mechanics 89 (2019) 93–101.

[39] W. Coppel, Stability and Asymptotic Behavior of Differential Equations, D. C. Heath and Company, Boston, 1965.

[40] R. Halir, J. Flusser, Numerically stable direct least squares fitting of ellipses, in: Proc. 6th International Conference in Central Europe on Computer Graphics and Visualization. WSCG, Vol. 98, Citeseer, 1998, pp. 125–132.

[41] D. Hildenbrand, Foundations of Geometric Algebra Computing, Springer Science and Business Media, 2013.